Parametric statistics of the scattering matrix: From metallic to insulating quasi-unidimensional disordered systems

E. R. Mucciolo [(1)], R. A. Jalabert [(2,3)], and J.-L. Pichard [(2,4)]

[(1)] *Departamento de Física, Pontifícia Universidade Católica, C.P. 38071, 22452-970 Rio de Janeiro, RJ, Brazil*

[(2)] *Institute for Theoretical Physics, University of California, Santa Barbara, CA 93106-4030*

[(3)] *Université Louis Pasteur, IPCMS-GEMME, 23 rue du Loess, 67037 Strasbourg Cedex, France*

[(4)] *Service de Physique de l'Etat Condensé, CEA Saclay, 91191 Gif-sur-Yvette, France*

(February 1, 2008)

Abstract

We investigate the statistical properties of the scattering matrix S describing the electron transport through quasi-one dimensional disordered systems. For weak disorder (metallic regime), the energy dependence of the phase shifts of S is found to yield the same universal parametric correlations as those characterizing chaotic Hamiltonian eigenvalues driven by an external parameter. This is analyzed within a Brownian motion model for S, which is directly related to the distribution of the Wigner-Smith time delay matrix. For large disorder (localized regime), transport is dominated by resonant tunneling and the universal behavior disappears. A model based on a simplified description of the localized wave functions qualitatively explains our numerical results. In the insulator, the parametric correlation of the phase shift velocities follows the energy-dependent autocorrelator of the Wigner time. The Wigner time and the conductance are correlated in the metal and in the insulator.

PACS numbers: 72.15.-v, 73.20.Dx, 72.10.Bg, 05.60.+w

Typeset using REVTEX

I. INTRODUCTION

A. Preface

Electron transport through quasi-one dimensional disordered systems is characterized by the scattering matrix S, relating the amplitudes of incoming and outgoing waves. The scattering matrix contains information about not only quantities as the conductance and the characteristic dwelling times for electrons moving through the disordered region, but also on the energy levels of the system. The universal statistical properties found in the energy spectrum of disordered and chaotic systems have been related to the distribution of eigenvalues of random matrix Hamiltonians [1–3]. On the other hand, the universal conductance fluctuations of metallic systems have been understood in terms of a statistical description of the transfer matrix [4,5]. To understand the relation between these two universalities, it is useful to study the statistical properties of the scattering matrix [6–11].

Due to current conservation, the scattering matrix is unitary and its eigenvalues are represented by $2N$ phase shifts $\{\theta_l\}$. (N is the number of transverse channels in each asymptotic region.) Assuming that all matrices S with a given symmetry are equally probable, we obtain Dyson's circular ensembles [12,13] (named COE and CUE for orthogonal and unitary symmetry classes, respectively), where the phase shift statistics follows universal laws. The isotropy hypothesis of Dyson's ensembles applies only to ballistic chaotic cavities with no direct channels [14,8], where the electronic motion is essentially zero-dimensional after a (short) time of flight. The conductance in this systems is always of the order of $N/2$ since reflection and transmission are equally likely. On the other hand, in disordered systems this isotropy hypothesis is not satisfied any longer because transmission is much less probable than reflection. For quasi-one-dimensional (quasi-1d) metallic samples the conductance is of the order of Nl/L, where l is the elastic mean-free-path, L the length of the disordered region, and $l \ll L$. In the localized regime, when the localization length $\xi \sim Nl$ is much smaller than the sample length L, the typical conductance scales as $\exp(-2L/\xi)$. However, the failure of Dyson's hypothesis for the mean values of S (which is linked to the average conductance) does not prevent the fluctuations of S for weakly-disordered quasi-1d samples to be (approximately) described with the universal behavior of the circular ensembles, as shown in Ref. [11]. This good agreement gets poorer if the disorder is increased, as well as when the system does not have a quasi-1d geometry, or when it enters the localized regime. In the first two cases the mean values of the transmission and reflection amplitudes become strongly dependent on the channel index and the eigenphase distribution is highly anisotropic. When localization is achieved by keeping the disorder weak and increasing the length of the sample beyond the localization length, the scattering matrix was shown to decouple in two statistically independent (almost unitary) reflection matrices [11]. This picture is particularly clear if one uses a semiclassical approach where most of the classical trajectories return to the region of departure instead of traversing the disordered sample.

A few years ago, another type of universality in the spectrum of chaotic and disordered systems was discovered by Szafer, Altshuler, and Simons [15,16]. It concerns the adiabatic response to an external perturbation (magnetic field, shape of the confining potential, etc). The correlator of the derivatives of the eigenenergies at two different values of the external parameter has a universal functional form once a proper rescaling is carried out. Latter

studies have found these universal parametric correlations to hold in a variety of other systems, including interacting one-dimensional models [17], $\vec{k}$-dependent band structures of semiconductors [18], Rydberg atoms in magnetic fields [19], etc. Considering the $2N$ eigenphases of S as a function of the electron energy, the natural question arises as to whether the analogous parametric correlations will have the universal form found for eigenenergies. In the weakly-disordered quasi-1d case, where the fluctuations of the eigenphases follow the circular ensemble predictions and $N \gg 1$, one could anticipate that the parametric correlations do exhibit the universal form of Szafer *et al.*, and this is confirmed here by numerical simulations and analytical arguments. More interesting is the question of what happens to these correlations as we go into the localized regime, and whether or not they can be described by a simple model as that of the decoupling of the eigenphases.

Directly related to the parametric correlations of the eigenphases, there is the question of the statistical distribution of the traversing-times in the disordered region. This distribution and the related correlation functions have recently begun to be addressed in Refs. [20,21], because the Wigner time appears in a variety of physical phenomena, ranging from the capacitance of mesoscopic quantum dots [22] to nuclear resonances [23]. Since the Wigner time is obtained from the scattering matrix and its energy derivative, the statistical properties of $S(E)$ determine the correlations of the traversal time. We aim in this paper to study the relationship between the parametric correlations and the distributions of the traversal times, and their connection to the statistical properties of the corresponding scattering matrix for metallic and localized quasi-1d disordered systems.

In the remaining of this section we introduce the basic notation concerning the scattering matrix and present the substantially different behavior of the eigenphases, conductance, and Wigner time (as functions of the Fermi energy) between the metallic and localized cases. In Sec. II we study the parametric correlations of weakly-disordered quasi-1d systems. We justify their universal character in the framework of a Brownian-motion model for unitary matrices. We then study the energy correlations of the conductance and the Wigner time and the cross-correlation between these two quantities, making contact with existing calculations in the metallic regime. In Sec. III we undertake similar studies for the localized regime. The non-universal parametric correlations of eigenphases and Wigner times can be accounted for, at the semi-quantitative level, by a very simple model of resonant transmission through a single localized state. We present our conclusions in Sec. IV. In Appendix A, we discuss the validity of the assumption on which is based the Brownian motion model, when it is used to describe the energy dependence of S. In this case, this amounts to study the underlying Wigner-Smith time delay matrix. In Appendix B we consider the simple case of one-channel scattering, where some exact calculations can be carried out.

B. Scattering matrix of a disordered region

We consider an infinite stripe composed of two semi-infinite, perfectly conducting regions of width L_y (which we define as the leads) connected by a disordered region of same width and of longitudinal length L_x (see the inset in Fig.1.a). Assuming non-interacting electrons and hard-wall boundary conditions for the transverse part of the wave function, the scattering states in the leads at the Fermi energy satisfy the condition $k^2 = (n\pi/L_y)^2 + k_n^2$, where k is the

Fermi wave vector, $n\pi/L_y$ the quantized transverse wave vector, and k_n the longitudinal wave vector. For a given k, each real transverse momenta labeled by the index n ($n = 1, \ldots, N$) define a propagating channel in the leads. Since each channel can carry two waves traveling in opposite directions, in regions asymptotically far from the scattering region the wave function can be specified by a two $2N$-component vectors, one for each lead (labeled I and II). For both vectors, the first (last) N components are the amplitudes of the waves propagating to the right (left). In mathematical terms, this reads

$$\Psi_I(x, y) = \sum_{n=1}^{N} \frac{1}{k_n^{1/2}} \left[A_n e^{ik_n x} + B_n e^{-ik_n x} \right] \phi_n(y) \tag{1.1a}$$

and

$$\Psi_{II}(x, y) = \sum_{n=1}^{N} \frac{1}{k_n^{1/2}} \left[C_n e^{ik_n (x-L_x)} + D_n e^{-ik_n (x-L_x)} \right] \phi_n(y). \tag{1.1b}$$

The transverse wave functions are $\phi_n(y) = \sqrt{2/L_y} \, \sin(\pi n y / L_y)$. The normalization is chosen in order to have a unit incoming flux on each channel. The scattering matrix S relates the incoming flux to the outgoing flux,

$$\begin{pmatrix} B \\ C \end{pmatrix} = S \begin{pmatrix} A \\ D \end{pmatrix}. \tag{1.2}$$

With this convention, S is a $2N \times 2N$ matrix of the form

$$S = \begin{pmatrix} r & t' \\ t & r' \end{pmatrix}. \tag{1.3}$$

The reflection (transmission) matrix r (t) is an $N \times N$ matrix whose elements r_{ba} (t_{ba}) denote the reflected (transmitted) amplitude in channel b when there is a unit flux incident from the left in channel a. The amplitudes r' and t' have similar meanings, except that the incident flux comes from the right.

The transmission and reflection amplitudes from a channel a on the left to a channel b on the right and left, respectively, are given by [24]

$$t_{ba} = -i\hbar (v_a v_b)^{1/2} \int dy' \int dy \, \phi_b^*(y') \, \phi_a(y) \, G_k(L_x, y'; 0, y) \tag{1.4a}$$

and

$$r_{ba} = \delta_{ab} - i\hbar (v_a v_b)^{1/2} \int dy' \int dy \, \phi_b^*(y') \, \phi_a(y) \, G_k(0, y'; 0, y), \tag{1.4b}$$

where v_a (v_b) is the longitudinal velocity for the incoming (outgoing) channel a (b). For hard-wall boundary conditions, $v_\alpha = \hbar k_\alpha / m$, $\alpha = a, b$. We denote by m the effective mass of the electrons. For the transmission (reflection) amplitudes $G_k(\mathbf{r}'; \mathbf{r})$ is the retarded Green's function between points $\mathbf{r} = (x, y)$ on the left lead and $\mathbf{r}' = (x', y')$ on the right (left) lead evaluated at the Fermi energy $E = \hbar^2 k^2 / 2m$. Note that, with the convention we have taken above, for a perfect, non-disordered sample at zero magnetic field, S is not the

identity matrix, but is rather written in terms of transmission submatrices which contain pure phases: $t_{ba} = t'^*_{ba} = \delta_{ab} \exp(ik_b L_x)$. Since we can pass from one convention to the other by a fixed unitary transformation, both forms present the same statistical properties [11].

In our numerical work we obtain the transmission and reflection amplitudes from the Green's function of the disordered stripe by a recursive algorithm [25,26] on a tight-binding lattice. We typically use a rectangular lattice of 34×136 sites and go from the metallic to the localized regime by increasing the on-site disorder W. (For details of the simulation see Ref. [11].)

From the transmission amplitudes one can obtain the two-terminal conductance through the Landauer formula [27]

$$g = \text{Tr}\,(tt^\dagger). \tag{1.5}$$

Here we adopt units of e^2/h for the conductance. (Throughout this work we will treat spinless electrons and therefore will not include spin-degeneracy factors.) Notice that the Landauer formula requires that the sample is a single, complex elastic scatterer. Thus, we are ignoring any inelastic process giving rise to a loss of phase coherence.

C. Eigenphases, conductance, and Wigner time in the metallic and localized regimes

For a given sample (i.e., impurity configuration) the diagonalization of the scattering matrix leads to $2N$ phase shifts $\{\theta_l\}$ as functions of the Fermi energy E. The typical dependence is shown in Fig. 1 for the metallic (a) and localized (b) cases for an energy interval where new channels are not open ($N = 14$ in the whole interval). In the metallic case the on-site disorder in Anderson units is $W = 1$, yielding a mean-free-path $l = 0.2L_x$, a localization length $\xi = 3L_x$, and a conductance (thick solid line) which fluctuates around a mean value $\langle g \rangle = 4.14$.

The localized regime ($W = 4$, yielding $l = 0.02L_x$ and $\xi = 0.3L_x$) exhibits a markedly different behavior, with phase shifts showing step-like jumps where the conductance has peaks. The peaks indicate that, for certain energies, the probability of traversing the disordered region is much higher than the average. They are related to the existence of localized eigenstates in the sample and transport through the strongly-disordered region is dominated by resonant tunneling.

To illustrate this last point, in Fig. 1 we also show the Wigner time for both metallic and localized regimes (thick dashed lines). This characteristic time scale is defined as the trace of the Wigner-Smith matrix

$$Q = \frac{\hbar}{2iN}\, S^\dagger(E)\, \frac{dS(E)}{dE}, \tag{1.6}$$

namely,

$$\tau_W \equiv \text{Tr}\,(Q). \tag{1.7}$$

The unitarity of S trivially implies the fact that Q is Hermitian, and therefore its eigenvalues are real. In the case of time-reversal symmetry $S^{\text{T}} = S$, but Q is not necessarily symmetric

since in general $S^\dagger$ and dS/dE do not commute. Working in a base that diagonalizes S it is easy to see that τ_W admits a simple expression in terms of the energy derivatives of the phase shifts,

$$\tau_W(E) = \frac{\hbar}{2N} \sum_{l=1}^{2N} \frac{d\theta_l(E)}{dE}. \tag{1.8}$$

The Wigner time can be interpreted as the typical time interval a scattered particle remains in the disordered region [20,11]. In the localized regime, the Wigner time exhibits the same resonant-like structure of the conductance, although peak heights can be relatively different. This behavior can be understood in the light of the resonant-tunneling mechanism, since each localized state present in the disordered region can trap the electrons for a long time [28]. From this mechanism one can also understand qualitatively why a Wigner-time peak can be relatively large when, at the same energy, a conductance peak is small. This may happen, for instance, when the tunneling probability rates for channels in lead I is much larger than for channels in lead II. We will get back to this discussion in Sec. III.

A strong correlation between g and τ_W is also obtained in the metallic regime. The correlation in this case is also intuitive, since transport should probe the available density of states around the considered Fermi energy.

II. CORRELATIONS IN THE METALLIC REGIME

A. Parametric correlations of eigenphases

In order to characterize the parametric dependence on energy of the set $\{\theta_l\}$, we define the *eigenphase* velocity correlator function

$$C_\theta(\Delta E) \equiv \left(\frac{N}{\pi}\right)^2 \left[\left\langle \frac{d\theta_l(E + \Delta E)}{dE} \frac{d\theta_l(E)}{dE} \right\rangle - \left\langle \frac{d\theta_l(E)}{dE} \right\rangle^2 \right], \tag{2.1}$$

together with the rescaling

$$x \equiv \Delta E \sqrt{C_\theta(0)} \tag{2.2a}$$

$$c_\theta(x) \equiv C_\theta(\Delta E)/C_\theta(0). \tag{2.2b}$$

The average $\langle \cdots \rangle$ can be performed over different eigenstates n, over the energy E, or over different realizations of disorder. These definitions are analogous to the well-studied case [15] in which a Hamiltonian H and its eigenvalues $\{\varepsilon_\nu\}$ depend on an external parameter ϕ (say, a magnetic flux) and the *eigenenergy* velocity correlator is given by

$$C_\varepsilon(\Delta\phi) \equiv \frac{1}{\Delta^2} \left[\left\langle \frac{d\varepsilon_\nu(\phi + \Delta\phi)}{d\phi} \frac{d\varepsilon_\nu(\phi)}{d\phi} \right\rangle - \left\langle \frac{d\varepsilon_\nu(\phi)}{d\phi} \right\rangle^2 \right], \tag{2.3}$$

where Δ denotes the mean level spacing, or inverse density of states around the ν-th eigenvalue. For chaotic systems, the universal form of this correlator was checked numerically from exact diagonalizations of suitable Hamiltonians [15,16] and after the rescaling

6

$$x \equiv \Delta\phi \ \sqrt{C_\varepsilon(0)} \tag{2.4a}$$
$$c_\varepsilon(x) \equiv C_\varepsilon(\Delta\phi)/C_\varepsilon(0). \tag{2.4b}$$

A complete analytical expression for $c_\varepsilon(x)$ is not available. However, the small and large-x asymptotic limits are known exactly from diagrammatic and non-perturbative calculations [15,16] and match accurately the numerical results. In particular, one finds that

$$c_\varepsilon(x) \longrightarrow -\frac{2}{\beta(\pi x)^2} \qquad \text{for} \qquad x \to \infty, \tag{2.5}$$

where $\beta = 1(2)$ for spinless systems with preserved (broken) time-reversal symmetry.

In Fig. 2 we present the eigenphase velocity correlation [Eq. (2.1)] resulting from our numerical simulations and the rescaling (2.2). For weakly-disordered, metallic samples where the statistics of the eigenphases at a fixed energy is well described by the Dyson circular ensembles [11], we obtain a good agreement with the universal parametric correlation found in Hamiltonian systems [15,16]. Applying a magnetic field perpendicularly to the stripe, one breaks the time-reversal symmetry, causing the parametric correlation behavior to go from GOE-like (squares) to GUE-like (circles) [29]. Increasing the disorder (but still remaining in the metallic regime) reduces the range of agreement with the universal curve. Further increase of the disorder drives the system into the localized regime and away from the universal behavior, as we will discuss in the Section III.

The system-independent form of parametric correlations for energy eigenvalues of random Hamiltonians has been studied with a non-linear σ model [30]. This treatment has been recently extended [31] to show that universality is a property of all systems whose underlying classical dynamics is chaotic. For a disordered sample, one finds that universality holds when $g \gg 1$ and the regime is metallic. The same approach has also been used to study the statistical fluctuations of the S matrix [32,21] and the conductance [10] of chaotic systems under the influence of a *generic* external parameter. However, there has been no attempt to prove analytically the results shown in Fig. 2, namely, that the *energy* correlator of eigenphase velocities falls into the analogous curve obtained from energy eigenvalues when the number of channels is very large.

Parallel to the field-theoretical approach, the universality of parametric correlators of eigenvalues has also been justified from the hypothesis of a Brownian motion of the eigenenergies [33], with the external parameter playing the role of a fictitious time. The Brownian-motion model (BMM) for Hermitian and unitary matrices was introduced by Dyson [34,13] and used by Pandey and collaborators [35] in the case of circular ensembles in order to determine the statistics of the eigenphases at the crossover between different symmetry classes. More recently, the BMM has been applied to scattering and transmission matrices describing coherent transport through chaotic and disordered systems [36,37]. It has been recognized in these works that the BMM approach for scattering matrices only obtains correct results for a restricted (energy or magnetic field) range, or for sufficiently large number of channels. We will illustrate this point in the next subsection, where we consider specifically the energy evolution of the phase shifts.

B. Brownian-motion model of S and energy-dependent parametric correlators

The aim of this subsection is to develop a simple description of the parametric statistics of phase shifts in the metallic regime numerically investigated ($N \gg 1$). For this purpose, we apply a Brownian-motion model to the energy evolution of scattering matrices. As stated at the end of the previous subsection, we do not expect to obtain a complete quantitative agreement between the BBM predictions and the numerical data - this certainly would require a more sophisticated treatment [6]. Instead, we only give a justification for the agreement observed between the asymptotics of the energy-dependent eigenphase correlation functions and analogous curves characteristic of Hamiltonian eigenvalues.

A unitary matrix S can always be decomposed as the product

$$S = Y' \, Y \tag{2.6}$$

of two unitary matrices. In the absence of time-reversal symmetry ($\beta = 2$), S is just unitary and Y and Y' are independent. For time-reversal symmetric systems ($\beta = 1$), $S = S^{\mathrm{T}}$ and we have $Y' = Y^{\mathrm{T}}$, where the matrix Y is not unique, but specified up to an orthogonal transformation. Any permissible small change in S is then given by

$$\delta S = Y' \, (i \delta \tilde{H}) \, Y, \tag{2.7}$$

where $\delta \tilde{H}$ is a Hermitian matrix (real symmetric if $\beta = 1$). This relationship allows us to define an invariant measure in the manifold of unitary matrices from the real independent components of $\delta \tilde{H}$ [12,13]. The isotropic Brownian motion of S occurs when S changes to $S + \delta S$ as some parameter (say, a fictitious time) varies from t to $t + \delta t$. To construct the model, the components of $\delta \tilde{H}$ are assumed to be independent random variables behaving according to

$$\langle \delta \tilde{H}_\mu \rangle = 0 \tag{2.8a}$$

and

$$f \langle \delta \tilde{H}_\mu \delta \tilde{H}_\nu \rangle = g_\mu \, \frac{\delta t}{\beta} \, \delta_{\mu\nu}, \tag{2.8b}$$

with $g_\mu = 1 + \delta_{ij}$ and $\mu = 1, \ldots, 2N + N(2N-1)\beta$. As it will be discussed in Appendix A, when the evolution of S results from a Fermi energy variation δE, the Hermitian matrix $\delta \tilde{H}$ can be given in terms of the Wigner-Smith time delay matrix Q. Thus, the validity of this Brownian motion model relies on certain assumptions concerning the statistical properties of the various interaction times. A random matrix approach for Q, assuming a maximum entropy distribution for a given mean density of eigenvalues, is proposed and some of its consequences are numerically checked. Eqs. (2.8) are then based on certain simplifications which we critically discuss in Appendix A, at the light of the statistical properties of the Wigner-Smith matrix Q.

The effect of the Brownian motion on the eigenphases of S may be found by second-order perturbation theory,

$$\delta\theta_n = \delta\tilde{H}_{nn} + \frac{1}{2}\sum_{m\neq n}(\delta\tilde{H}_{mn})^2 \ \cot\left(\frac{\theta_n - \theta_m}{2}\right). \tag{2.9}$$

Equations (2.8) and (2.9) then imply that the eigenphases follow the relations

$$\langle\delta\theta_n\rangle = \frac{1}{f} \ F(\theta_n) \ \delta t \tag{2.10a}$$

and

$$\langle\delta\theta_n\delta\theta_m\rangle = \delta_{nm} \ \frac{2}{f\beta} \ \delta t, \tag{2.10b}$$

with $F(\theta_n) \equiv -\partial W/\partial\theta_n$ and $W = -\sum_{n<m}\ln|2\sin[(\theta_n - \theta_m)/2]|$. Notice that the coefficients f and β were introduced to suggest friction and inverse temperature, respectively. The eigenphases behave like a classical gas of massless particles on the unit circle, executing a Brownian motion under the influence of a Coulomb force F. The joint probability distribution of the eigenphases $P(\{\theta_n\}; t)$ follows a Fokker-Planck equation [34,13]

$$\frac{\partial P}{\partial t} = \frac{1}{f} \ \sum_{n=1}^{2N} \frac{\partial}{\partial\theta_n}\left(\frac{1}{\beta}\frac{\partial P}{\partial\theta_n} + P\frac{\partial W}{\partial\theta_n}\right). \tag{2.11}$$

For $t \to \infty$ we reach an equilibrium situation where the joint distribution becomes that of the circular ensemble [13], $P_{eq}(\{\theta_n\}) = C_{2N}\exp[-\beta W(\{\theta_n\})]$.

We now turn to the solution of the Fokker-Planck equation for the joint probability distribution of the eigenphases. An exact way to solve Eq. (2.11) is to map it into a quantum-mechanical Hamiltonian problem of particles in a ring interacting by a two-body potential proportional to $1/r_c^2$, where r_c^2 is the length of the chord connecting the pair. This model was proposed and studied extensively by Sutherland [38] and yields an exact solution for $P(\{\theta_n\}; t)$ [39]. Alternatively, one may use a hydrodynamical approximation, originally proposed by Dyson [40], which leads to a non-linear diffusion equation for the average density of eigenphases. Here we will adopt this second approach, since it is simpler than the first one and sufficient for our purposes. Thus, introducing the t-dependent density of eigenphases,

$$\rho(\theta; t) \equiv \int_0^{2\pi} d\theta_1 \cdots d\theta_{2N} P(\{\theta_l\}; t)\sum_{n=1}^{2N}\delta(\theta - \theta_n), \tag{2.12}$$

and starting from Eq. (2.11), one can derive that

$$f\frac{\partial\rho(\theta; t)}{\partial t} = -\frac{\partial}{\partial t}\left[\rho(\theta; t)\frac{\partial}{\partial\theta}\int_0^{2\pi} d\theta'\rho(\theta'; t)\ln\left|2\sin\left(\frac{\theta - \theta'}{2}\right)\right|\right]. \tag{2.13}$$

(This equation is approximate in the sense that it does not take into account accurately short-wavelength oscillations in the density.) Since fluctuations in the density are smaller than the density itself by a factor of the order $O(1/N)$, one can linearize this diffusive equation by considering small deviations around the homogeneous solution, $\rho(\theta; t) = \rho_{eq} + \delta\rho(\theta; t)$, where $\rho_{eq} = N/\pi$. One then obtains

9

$$\frac{\partial \delta\rho(\theta;t)}{\partial t} = \frac{\partial}{\partial \theta} \int_0^{2\pi} d\theta' D(\theta - \theta') \frac{\partial \delta\rho(\theta';t)}{\partial \theta'}, \tag{2.14}$$

where the kernel is given by $D(\theta) = -\rho_{eq} f^{-1} \ln |2\sin[(\theta - \theta')/2]|$. The periodicity in the eigenphase space calls for a solution of the diffusion equation in Fourier series. Writing $\delta\rho(\theta;t) = \sum_{k=-\infty}^{+\infty} \delta\rho_k(t) e^{ik\theta}$, one finds that

$$\delta\rho_k(t) = \delta\rho(0) \exp\left(-\frac{\pi|k|\rho_{eq}t}{f}\right). \tag{2.15}$$

The above result can be readily used in the evaluation of parametric correlators, which will be the subject of the rest of this subsection. We therefore introduce the two-point density correlator

$$R(\theta, \theta'; t, t') \equiv \langle \delta\rho(\theta;t)\delta\rho(\theta';t') \rangle_{eq}, \tag{2.16}$$

where $\langle \cdots \rangle_{eq}$ means that the average is weighted by the joint distribution at the equilibrium, $P_{eq}(\{\theta_l\})$. Since the average density is constant in both time and angle, there is translation invariance in t and θ at the equilibrium. Consequently, R depends only on the differences $\theta - \theta'$ and $t - t'$). From Eq. (2.15), we find that the dependence on time and angle can be decoupled in $k-$space,

$$R_k(t) = T_k \exp\left(\frac{-\pi|k|\rho_{eq}t}{f}\right), \tag{2.17}$$

where T_k is the Fourier coefficient of the "static" correlator $T(\theta) \equiv R(\theta; t = 0)$, which, for circular ensembles, is known exactly [13]. In the limit of $N \gg 1$, one has that $T_k \simeq |k|/(2\pi^2\beta)$ for $|k| \ll N$, whereas for $|k| \gg N$ it saturates at the value $T_k \simeq N/(2\pi)^2$. If we keep $\pi\rho_{eq}t/f \gg 1/N$, we can neglect the contribution of terms with $|k| > N$ and then easily sum the Fourier expansion of $R(\theta; t)$ to find that

$$R(\theta; t) \simeq \frac{1}{\pi^2\beta} \text{Re}\left[\frac{z}{(1-z)^2}\right], \tag{2.18}$$

with $z = \exp(i\theta - \pi\rho_{eq}t/f)$. Hereafter we will denote the energy (or time) in terms of a dimensionless parameter, with the natural choice being $X \equiv E/E_s$, where $E_s = \sqrt{f/(\pi\rho_{eq})}$.

The knowledge of $R(\theta; t)$ permits the evaluation of other two-point parametric functions. Two of them are of particular interest. The first one is the Wigner time correlator

$$C_\tau(\Delta E) \equiv \langle \tau_W(E + \Delta E)\tau_W(E) \rangle - \langle \tau_W(E) \rangle^2$$
$$= \left(\frac{\hbar}{2N}\right)^2 \sum_{l,m=1}^{2N} \left[\left\langle \frac{d\theta_l(E + \Delta E)}{dE} \frac{d\theta_m(E)}{dE} \right\rangle - \left\langle \frac{d\theta_l(E)}{dE} \right\rangle \left\langle \frac{d\theta_m(E)}{dE} \right\rangle\right], \tag{2.19}$$

which has also been the subject of recent calculations [20,21]. The second parametric function is the modified level velocity correlator [16,33]

$$\tilde{C}(\theta - \theta'; E - E') \equiv \sum_{n,m=1}^{2N} \left\langle \frac{d\theta_n(E)}{dE} \frac{d\theta_m(E')}{dE'} \delta(\theta - \theta_n(E))\delta(\theta' - \theta_m(E')) \right\rangle_{eq}. \tag{2.20}$$

It is straightforward to check that

$$C_\tau(E) = -\frac{\pi}{(2N)^2}\frac{\partial^2}{\partial E^2}\int_0^{2\pi} d\theta\,(\theta-\pi)^2 R(\theta;E) \tag{2.21}$$

and

$$\frac{\partial^2 R}{\partial E^2} = \frac{\partial^2 \tilde{C}}{\partial \theta^2}. \tag{2.22}$$

In Eq. (2.21) one uses that $R(\theta;E)$ is an even periodic function in θ and $R_k(E) = 0$ for $k = 0$.] Moreover, the two correlators are connected by the relation

$$C_\tau(E) = \frac{2\pi}{(2N)^2}\int_0^{2\pi} d\theta\,\tilde{C}(\theta;E), \tag{2.23}$$

which also implies that $\tilde{C}(0;E) = 2(N/\pi)^2 C_\tau(E)$.

Two remarks are pertinent here. First, $C_\tau(E)$ and $\tilde{C}(0;E)$ have asymptotic forms similar to $C_\theta(E)$ in the limit of large E. This is because distinct eigenphases become uncorrelated very quickly for large enough energy differences, causing the main contribution to both correlators to come from the diagonal terms. The second remark is that, independently of the hydrodynamic approximation adopted above, interlevel correlations are completely ignored in the BBM [see Eq. (2.10b)]. This leads to a $C_\tau(E)$ identical, up to a proportionality factor, to the one-level velocity correlator $C_\theta(E)$ *for all values of E*. Such a coincidence between $C_\tau(E)$ and $C_\theta(E)$ is never observed in practice because interlevel correlations are indeed important, particularly among neighboring levels and at small values of E.

From Eqs. (2.17), (2.21), and (2.22) one gets

$$C_\tau(E) = -\frac{1}{2\beta N^2 E_s^2}\frac{(e^{-X^2}-1+2X^2)}{\sinh^2(X^2/2)} \tag{2.24}$$

and

$$\tilde{C}(\theta;E) = \left(\frac{N}{\pi}\right)^2 C_\tau(E) - \frac{2}{\pi^2\beta E_s^2}\mathrm{Re}\left[\frac{z^2-z(1-2X^2)}{(1-z)^2}\right]. \tag{2.25}$$

We find the following asymptotic limits: (*i*) For $X \ll 1$, $C_\tau(E) \simeq -2/(\beta N^2 E^2)$ and $\tilde{C}(0;E) \simeq -4/(\pi^2\beta E^2)$; (*ii*) for $X \gg 1$, $C_\tau(E) \simeq -4X^2 e^{-X^2}/(\beta N^2 E_s^2)$ and $\tilde{C}(0;E) \simeq -8X^2 e^{-X^2}/(\pi^2\beta E_s^2)$. An exponential decay at large distances does not occur for the analogous correlators involving eigenvalue velocities [33], which actually retains the form (*i*) for arbitrarily large values of the external parameter. As pointed out before [37], technically, the difference appears because a Fourier series is used to treat phase shifts oscillations (since they are bounded by the finite interval $[0;2\pi]$) instead of Fourier transforms, as in the case of energy eigenvalues. Nevertheless, if $N \gg 1$, one naturally expects that there should exist a range of values of E in which $\tilde{C}(\theta;E)$ has a form similar to its counterpart for eigenenergies. In order to understand this point, let us find the relation between E_s and another, more commonly used scale, $C_\theta(0)^{-1/2}$ [15,16] (see Sec. II A). From Eq. (2.10b) we have that

11

$$C_\theta(0)^{-1/2} = \frac{1}{\rho_{eq}}\sqrt{\frac{f\beta}{2}}. \tag{2.26}$$

which means that $E_s = C_\theta(0)^{-1/2}\sqrt{2N/(\pi^2\beta)}$. Therefore, if N is large enough, it is possible to have $E \gg E_s$ and $E \ll C_\theta(0)^{-1/2}$ simultaneously. Consequently, there is an intermediate range of values of X where $\tilde{C}(0; X)$ falls exactly into the same power-law, universal curve predicted for the case of energy eigenvalues [16,33]. Deviations in the form of an exponential decay occur only for values of $X \gtrsim 1$, which may be large in units of $C_\theta(0)^{-1/2}/E_s$. Notice that this is still compatible with the restriction $E/E_s \gg 1/N$ used to derive Eq. (2.18).

We stress again that Eqs. (2.24) and (2.25) are approximations. A simple inspection is sufficient to prove this point: Because the correlators diverge at $E = 0$ as $1/E^2$, they cannot satisfy the sum rules $\int_0^\infty dE \ \tilde{C}(\theta; E) = 0$ (for any θ) and $\int_0^\infty dE \ C_\tau(E) = 0$. This limitation cannot be overcome within the hydrodynamical approximation we have considered here. In fact, Eqs. (2.24) and (2.25) break down for $X \lesssim C_\theta(0)^{-1/2}$. To go beyond this limitation, one has to treat Eq. (2.11) in a non-perturbative way.

There is an additional, appealing relation connecting E_s to another scale inherent to the scattering region. Recall that $E_s = (\hbar/N)/\sqrt{\beta(\langle\tau_W^2\rangle - \langle\tau_W\rangle^2)}$. The variance of the Wigner time was evaluated in Refs. [20,21] using a microscopic formulation to relate S to the Hamiltonian of the scattering region, which was modeled as a member of a Gaussian ensemble [6]. (We remind the reader that Gaussian ensembles are supposed to model the statistical properties of ballistic chaotic cavities as well as disordered electronic systems in the diffusive regime.) It was shown that

$$\langle\tau_W^2\rangle = \langle\tau_W\rangle^2\left[1 + \frac{4}{\beta(2N)^2}\right] \tag{2.27}$$

when the scattering region is maximally connected to the external propagating channel (i.e., open leads) and $N \gg 1$. Based on this result, we infer

$$E_s = \frac{N\Delta}{\pi}. \tag{2.28}$$

This relation says that in the metallic regime of a quasi-1D wire, only one fundamental energy scale, the mean level spacing, is required to characterize the decay of energy-parametric correlators. Other system-dependent scales, like the Thouless energy $E_c = \hbar v_F l/L^2$ are irrelevant. One should recall that, for energy levels, the analogous quantity to $C_\theta(0)^{-1/2}$ is the root-mean square velocity $C_\varepsilon(0)^{-1/2}$ [see Eq. (2.4)], which is a direct measure of the average dimensionless conductance $\langle g\rangle \sim E_c/\Delta$ *when the system is in the metallic regime* [16,45]. There is no direct relation between $C_\theta(0)^{-1/2}$ and $C_\varepsilon(0)^{-1/2}$ and one cannot recover any quantitative information about the conductance of the system by calculating $C_\theta(E)$ alone in the metallic regime.

In Fig. 3 we present the Wigner time correlator (2.19) with the energy rescaled according to Eq. (2.2). Notice that the shape of C_τ is very similar for different symmetry classes ($\beta = 1$ and 2). This property also emerges in the context of the stochastic approach to scattering [6] when we take the large-N asymptotics of C_τ [20,21]: The form of the correlator becomes

$$C_\tau(E) = C_\tau(0)\frac{1 - (E/\Gamma)^2}{[1 + (E/\Gamma)^2]^2},\tag{2.29}$$

with $\Gamma = N\Delta/\pi$. This curve matches reasonably well our data when we let Γ be a *free* fitting parameter.

From a semiclassical point-of-view, the existence of time-reversal symmetry *in a chaotic system* does not affect the shape of any energy-dependent, two-point correlator of elements of S [41,42] or τ_W [43]. This is because, after energy averaging, these correlators are solely determined by the exponential decay with time of the classical probability to escape from the scattering region, in which case Γ^{-1} is interpreted as the escape rate. The presence or not of time-reversal symmetry affects only numerical prefactors in the correlators. The fact that large N corresponds to a semiclassical limit becomes clear when we notice that taking $\hbar \to 0$ for a fixed lead geometry effectively increases the number of propagating channels [44].

C. Correlation between the Wigner time and the conductance

In the previous subsection we discussed the Brownian motion model for S and the importance of the probability distribution of the time-delay matrix (further developed in Appendix A). We now focus on the statistical properties of the trace of Q, the Wigner time τ_W in the metallic regime. As evident from Fig.1, there are strong correlations between the Wigner time and the conductance, that we discuss below. We start by writing the scattering matrix in its polar decomposition [4]

$$S = \tilde{U}\,\Gamma\,U.\tag{2.30}$$

The $2N \times 2N$ unitary matrices U and $\tilde{U}$ are built out of unitary $N \times N$ blocks, namely,

$$U = \begin{pmatrix} u^{(1)} & 0 \\ 0 & u^{(2)} \end{pmatrix} \quad\text{and}\quad \tilde{U} = \begin{pmatrix} u^{(3)} & 0 \\ 0 & u^{(4)} \end{pmatrix}.\tag{2.31}$$

For systems with broken time-reversal symmetry, the matrices $u^{(l)}$ are independent of each other. If time-reversal symmetry is preserved, then S is symmetric and one has $u^{(3)} = u^{(1)T}$ and $u^{(4)} = u^{(2)T}$. The $2N \times 2N$ matrix Γ has the block structure

$$\Gamma = \begin{pmatrix} -\mathcal{R} & \mathcal{T} \\ \mathcal{T} & \mathcal{R} \end{pmatrix},\tag{2.32}$$

where $\mathcal{R}$ and $\mathcal{T}$ are real diagonal $N \times N$ whose non-zero elements can be expressed as

$$\mathcal{R}_a = \left(\frac{\lambda_a}{1 + \lambda_a}\right)^{1/2} \qquad\text{and}\qquad \mathcal{T}_a = \left(\frac{1}{1 + \lambda_a}\right)^{1/2}\tag{2.33}$$

in terms of the radial parameters λ_a. The convenience of this representation is that it allows the two-probe conductance of Eq. (1.5) to be expressed simply as

$$g = \sum_{a=1}^{N} \frac{1}{1+\lambda_a}, \tag{2.34}$$

that is, independent of the unitary matrices U and $\tilde{U}$.

In the absence of a magnetic field there is time-reversal symmetry ($S = S^{\mathrm{T}}$, $\tilde{U} = U^{\mathrm{T}}$), and we have

$$S^{\dagger} \frac{dS}{dE} = U^{\dagger}\Gamma \left[\frac{d\Gamma}{dE}U + \Gamma\frac{dU}{dE} - \frac{dU^*}{dE}U^{\mathrm{T}}\Gamma U \right]. \tag{2.35}$$

Since $\Gamma^2 = I$, taking the trace of the above equation simplifies it, yielding

$$\tau_W(E) = -i\,\frac{\hbar}{2N}\,\mathrm{Tr}\left(U^{\dagger}\frac{dU}{dE} - \frac{dU^*}{dE}U^{\mathrm{T}} \right). \tag{2.36}$$

Moreover, because U is unitary, its infinitesimal variations are given by $dU = \delta U\,U$, where δU is antihermitian. Therefore,

$$\tau_W(E) = -i\,\frac{\hbar}{2N}\,\mathrm{Tr}\left(\frac{\delta U}{dE} - \frac{\delta U^*}{dE} \right). \tag{2.37}$$

Writing for the block components of U

$$du^{(l)} = \delta u^{(l)}\,u^{(l)} \quad \text{and} \quad \delta u^{(l)} = da^{(l)} + i\,ds^{(l)}, \tag{2.38}$$

$l = 1, 2$, where $da^{(l)}$ ($ds^{(l)}$) are real antisymmetric (symmetric) $N \times N$ matrices, we have

$$\tau_W(E) = -\frac{\hbar}{N}\sum_{l=1}^{2}\sum_{a=1}^{N}\frac{ds_{aa}^{(l)}}{dE}. \tag{2.39}$$

Notice that here $\langle \tau_W \rangle = 0$, since the polar decomposition (2.30) yields the identity for S in the absence of disorder. However, with the convention of Eq. (1.1) which we took for defining our scattering matrix in the numerical simulations, we do not have $S = I$ in the absence of disorder. As a consequence, the mean average value of the Wigner time obtained numerically is given by the density of states of the disordered region [11,46]. However, as expressed in Sec. I, when we go from one convention to another by multiplying S by a fixed unitary matrix, we do not change the statistical properties of the eigenphases. In the same way, the constant shift in τ_W given by the density of states does not change its statistical properties.

One interesting feature of Eqs. (2.37) and (2.39) is that τ_W only depends on the infinitesimal variations of the unitary matrix U and not on the radial parameters λ of the polar decomposition. This may seem somehow surprising, given the obvious correlations between the Wigner time and the conductance [as shown in Figs. 1.a and 3] and the fact that the latter depends exclusively on the radial parameters through Eq. (2.34). However, when the electron Fermi energy is varied for a given impurity configuration, the corresponding changes in λ and $\delta u^{(l)}$ are necessarily correlated since S is constrained by symmetry to move along a particular direction in the manifold of allowed polar parameters. In other words, since

the Wigner time is given by the energy derivative of S, it must comply with the symmetry requirements in the same way as the infinitesimal variations that define the invariant measure.

In Fig. 3 we present the $g - \tau$ correlator

$$C_{g\tau}(\Delta E) = \frac{\langle \delta g(E + \Delta E) \; \delta \tau_W(E) \rangle}{\langle (\delta g)^2 \rangle^{1/2} \langle (\delta \tau_W)^2 \rangle^{1/2}}, \tag{2.40}$$

together with the $g-g$ and $\tau - \tau$ correlators. (Here we define $\delta \tau_W \equiv \langle \tau_W^2 \rangle - \langle \tau_W \rangle^2$. Analogously for δg.) The correlator of Wigner times has been recently calculated by several authors [20,21] using supersymmetry methods, while the $g - g$ correlator is only known analytically in the metallic perturbative regime [47] when $E \gg \Delta$. The calculation of the $g - \tau$ correlator will be very interesting, given the numerical evidence provided.

III. CORRELATIONS IN THE LOCALIZED REGIME

A. Resonant transmission model for localized transport

As evident from Fig. 1, transport through a localized stripe presents important differences for the eigenphases, conductance, and Wigner time as compared to the metallic case of Section II. The peaks of $g(E)$ and $\tau_W(E)$ and the jumps of $\theta_l(E)$ show that now we are in a resonant regime, where the transmission occurs through tunneling into localized eigenstates in the bulk of the disordered region. The dependence of transport properties on resonant states can be established within the R-matrix formalism [48], which allows the scattering matrix to be expressed as [49] (see Appendix B)

$$S_{nm}(E) \simeq \delta_{nm} - 2\pi i \sum_{\nu} \frac{W_{n\nu}^* W_{m\nu}}{E - E_\nu + i\Gamma_\nu/2}. \tag{3.1}$$

The sum is over the (localized) eigenstates of the disordered region, the matrix elements $W_{m\nu}$ describe the coupling of these states with the different channels in the leads, and $\Gamma_\nu = 2\pi \sum_{n=1}^{2N} |W_{n\nu}|^2$ is the resonance total width for the eigenstate ν. Equation (3.1) is valid only to lowest order in Γ_ν/Δ, namely, when resonances do not overlap. (Higher order corrections imply traversing the disordered region by sequential tunneling through more than one localized state.) Within this approximation, the energy dependence of the conductance and the Wigner time appears in the form of Breit-Wigner functions

$$g(E) \simeq \sum_{\nu} \frac{\Gamma_\nu^{(l)} \Gamma_\nu^{(r)}}{(E - E_\nu)^2 + \Gamma_\nu^2/4} \tag{3.2}$$

and

$$\tau_W(E) \simeq \frac{\hbar}{2N} \sum_{\nu} \frac{\Gamma_\nu}{(E - E_\nu)^2 + \Gamma_\nu^2/4}, \tag{3.3}$$

respectively. The left ($\Gamma_\nu^{(l)}$) and right ($\Gamma_\nu^{(r)}$) partial widths are given by the overlap of the corresponding eigenfunction $\psi_\nu(x, y)$ with the channel wave functions $\phi_n(y)$, i.e.,

15

$$\Gamma_\nu^{(l)} = \Delta \sum_{n=1}^{N} c_n \left| \int_0^{L_y} dy \; \phi_n(y) \psi_\nu(x{=}0, y) \right|^2 \tag{3.4}$$

and similarly for $\Gamma_\nu^{(r)}$, exchanging $x = 0$ by $x = L$. The total width is $\Gamma_\nu = \Gamma_\nu^{(l)} + \Gamma_\nu^{(r)}$. The coefficients $c_n = \hbar^2 k_n / (2m\Delta)$ are smooth functions of energy on the scale of Δ (k_n is the longitudinal wave vector defined in Sec. I.B). In the strongly localized case assumed here, the typical total width Γ_ν is much smaller than Δ and only the eigenstate ν whose energy is the closest to E contributes significantly to the sum. Hence, from now on we will neglect any smooth energy dependence in Γ_ν and omit the index ν. The fitting of $g(E)$ by a single Breit-Wigner resonance works quite well for our numerical data when $W = 4$ or larger; other numerical models of disorder [50] also yield Breit-Wigner shapes.

The statistical properties of Γ are connected to the fluctuations in the eigenfunction intensity. Using some very simple arguments one can estimate the probability distribution $P(\Gamma)$. First we recall that the envelope of a localized state decays as one moves away from its center $r_0 = (x_0, y_0)$. The scale of this decay is the localization length ξ, such that $|\psi(r)| \sim \exp(-|r - r_0|/\xi)$. Consequently, we may write that

$$\Gamma^{(l)} \sim e^{-2x_0/\xi} \; f_N^{(l)}\{\psi\} \tag{3.5a}$$

and

$$\Gamma^{(r)} \sim e^{-2(L-x_0)/\xi} \; f_N^{(r)}\{\psi\}. \tag{3.5b}$$

The factors f_N arise from the fluctuations of the eigenstate on the scale of k_F^{-1}. However, since we work with a large number of channels N, f_N follows approximately a Gaussian distribution and therefore can be substituted by the its average value. Factorizing away the energy scale given by the level spacing Δ, we define

$$\gamma^{(l)} \equiv \frac{\Gamma^{(l)}}{c\Delta} \sim e^{-2x_0/\xi} \tag{3.6a}$$

and

$$\gamma^{(r)} \equiv \frac{\Gamma^{(r)}}{c\Delta} \sim e^{-2(L-x_0)/\xi}, \tag{3.6b}$$

where c is a numerical constant proportional to N. Analogously, we define the dimensionless total width $\gamma = \gamma^{(l)} + \gamma^{(r)}$.

Our statistical assumptions will be the following:

1. x_0 is uniformly distributed along the disordered stripe,

$$P(x_0) = \frac{1}{L}; \tag{3.7}$$

2. x_0 and ξ are independent random variables;

16

3. $z = 2L/\xi$ has a normal distribution [51]

$$P(z) = F \ \exp\left[-\frac{(z - z_0)^2}{2\sigma^2}\right],$$ (3.8)

where the mean and the variance are related by $\sigma^2 = 2z_0$. The two first assumptions are trivial. The third assumption originates from the standard log-normal distribution of the dimensionless conductance [51], $g = e^{-z}$, with

$$\mathrm{var}(\ln g) = -2 \ \langle \ln g \rangle.$$ (3.9)

The mean value z_0 is a measure of the disorder, and in the strongly localized regime we have $z_0 \gg 1$. The normalization factor $F = [\sqrt{\pi z_0}(1 + \Phi(\sqrt{z_0}/2))]^{-1}$ takes into account the fact that z is always positive. (Φ denotes the error function.) Nevertheless, to leading order in $1/z_0$, we can ignore this restriction over z and recover the standard Gaussian prefactor $F \simeq [2\sqrt{\pi z_0}]^{-1}$. The probability distribution of γ can be constructed as

$$P(\gamma) \simeq 2F \int_0^{1/2} ds \int_0^\infty dz \exp\left[-\frac{(z - z_0)^2}{4z_0}\right] \delta\Big(\gamma - 2e^{-z/2}\cosh(sz)\Big),$$ (3.10)

with $s = x_0/L - 1/2$. Carrying out one integration, we find that

$$P(\gamma) \simeq 2F \int_{z_1}^{z_2} \frac{dz}{z} \exp\left[-\frac{(z - z_0)^2}{4z_0}\right] \frac{1}{\sqrt{\gamma^2 - 4e^{-z}}},$$ (3.11)

with $z_1 = 2\ln(2/\gamma)$, $z_2 = +\infty$ if $0 < \gamma < 1$, or $z_2 = -\ln(\gamma - 1)$ if $1 < \gamma < 2$. We cannot simplify Eq. (3.11) further, and in Fig. 4 we show the result of a numerical integration. Obviously, our estimate of $P(\gamma)$ is accurate only when $\gamma \ll 1$. Working the various asymptotic limits, we see that for very small γ ($z_1 \gg z_0$), the probability distribution vanishes as

$$P(\gamma) \propto \frac{z_0}{z_1^{5/4}} \ \exp\left(-\frac{z_1^2}{4z_0}\right).$$ (3.12)

The distribution has a maximum around $\gamma_{mp} \simeq 2e^{-z/2}$, which becomes more pronounced for increasing disorder, namely,

$$P(\gamma_{mp}) \propto \frac{1}{z_0} \ \exp\left(\frac{z_0}{2}\right).$$ (3.13)

The large values of γ are not exponentially damped by disorder, as we have

$$P(\gamma \simeq 1) \propto \frac{1}{z_0}.$$ (3.14)

The knowledge of $P(\gamma)$ allows us to estimate various averages. For instance, let us show that the model is consistent. From the Breit-Wigner form of the conductance (3.2) we can write

$$\langle \ln g \rangle = \frac{1}{\Delta} \left\langle \int_{-\Delta/2}^{\Delta/2} dE \, \ln \left[\frac{\gamma^{(l)} \gamma^{(r)}}{(E/c\Delta)^2 + \gamma^2/4} \right] \right\rangle$$

$$= \left\langle \ln \left[\gamma^{(l)} \gamma^{(r)} \right] \right\rangle - \left\langle \ln \left(\frac{\gamma^2}{4} \right) \right\rangle - \left\langle \ln \left(\frac{1}{\gamma^2 c^2} + 1 \right) \right\rangle$$

$$+ 2 \left[1 - \left\langle \gamma c \, \arctan \left(\frac{1}{\gamma c} \right) \right\rangle \right], \tag{3.15}$$

with the averages taken with respect to $P(\gamma)$. The first term on the right-hand side gives the dominant contribution,

$$\left\langle \ln \left[\gamma^{(l)} \gamma^{(r)} \right] \right\rangle = \langle -z \rangle \simeq -z_0. \tag{3.16}$$

Since $P(z)$ selects values of $z \sim z_0 \gg 1$, the remaining terms of (3.15) give the next leading-order contribution, which is independent of z_0,

$$- \left\langle \ln \left[\left(\frac{\gamma}{2} \right)^2 \left(\frac{1}{\gamma^2 c^2} + 1 \right) \right] \right\rangle + 2 \simeq 2 \ln(2c) + 2. \tag{3.17}$$

The fluctuations of $\ln g$ are characterized by the correlation function

$$\mathcal{C}_g(\Delta E) = \langle \ln g(E + \Delta E) \ln g(E) \rangle - \langle \ln g(E) \rangle^2, \tag{3.18}$$

with the average running over energy E and disorder. Following the statistical assumptions introduced above, we have

$$\langle \ln^2 g \rangle = \frac{1}{\Delta} \left\langle \int_{-\Delta/2}^{\Delta/2} dE \, \ln^2 \left[\frac{\gamma^{(l)} \gamma^{(r)}}{(E/c\Delta)^2 + \gamma^2/4} \right] \right\rangle$$

$$\simeq \left\langle \ln^2 \left[\gamma^{(l)} \gamma^{(r)} \right] \right\rangle + \left\langle \ln^2 \left(\frac{\gamma^2}{4} \right) \right\rangle + 2 \left\langle \left\{ \ln \left[\gamma^{(l)} \gamma^{(r)} \right] - \ln \left(\frac{\gamma}{2} \right) \right\} \left[\ln \left(\gamma^2 c^2 \right) + 1 \right] \right\rangle$$

$$+ \left\langle \ln^2 \left(\gamma^2 c^2 \right) \right\rangle + 4 \left\langle \ln \left(\gamma^2 c^2 \right) \right\rangle$$

$$\simeq z_0^2 - 2 z_0 \left[2 \ln(2c) + 1 \right]. \tag{3.19}$$

The variance of the distribution of $\ln g$ is then given by $\mathcal{C}_g(\Delta E = 0) \simeq 2 z_0$, showing that our resonant model for localized transport is consistent with the standard log-normal distribution of the conductance [51] characterized by Eq. (3.9). In subsection III.C, we will apply the resonant model to the correlation function (3.18) and will determine its energy-correlation length.

B. Wigner time in the localized regime and correlations with the conductance

The resonant model can be applied to the Wigner time, whose average is given by

$$\langle \tau_W \rangle \simeq \frac{\hbar}{2N} \frac{1}{c\Delta^2} \left\langle \int_{-\Delta/2}^{\Delta/2} dE \left[\frac{\gamma}{(E/c\Delta)^2 + \gamma^2/4} \right] \right\rangle$$

$$\simeq \frac{\hbar}{2N} \frac{4}{\Delta} \left\langle \arctan \left(\frac{1}{\gamma c} \right) \right\rangle$$

$$\simeq \frac{\hbar}{2N} \frac{2\pi}{\Delta}. \tag{3.20}$$

18

This result also checks the consistency of our model. Notice that although τ_W fluctuates strongly with energy and from sample to sample, $\langle \tau_W \rangle$ essentially does not depend on disorder. This is due to the fact that the mean slope of the eigenphases as a function of energy is proportional to the density of states [11,46] (or equal to zero, depending on the particular convention adopted for S). Large values of τ_W at the resonances are compensated by the flat parts in between. These large fluctuations are not appropriately represented by the usual linear correlation function (2.19), which, within our resonant model, is given by

$$C_\tau(\Delta E) = \left(\frac{\hbar}{2N}\right)^2 \frac{4\pi}{c\Delta^2} \int_0^2 d\gamma \, \frac{P(\gamma)}{\gamma} \frac{1}{[\Delta E/(c\gamma\Delta)]^2 + 1} - \langle\tau_W\rangle^2. \tag{3.21}$$

In order to see why, we calculate the second moment of τ_W:

$$\begin{aligned}
\langle\tau_W^2\rangle &= \left(\frac{\hbar}{2N}\right)^2 \frac{8\pi}{c\Delta^2} \int_0^\infty dz \, \frac{P(z)}{z} \int_{\gamma_{\min}}^{\gamma_{\max}} \frac{d\gamma}{\gamma\sqrt{\gamma^2 - \gamma_{\min}^2}} \\
&\simeq \left(\frac{\hbar}{2N}\right)^2 \frac{2\pi^2}{c\Delta^2} \frac{1}{z_0} \exp\left(\frac{3}{4}z_0\right).
\end{aligned} \tag{3.22}$$

The lower and upper limits of γ for a given z are $\gamma_{\min} = 2e^{-z/2}$ and $\gamma_{\max} = 1 + e^{-z}$. In obtaining the above result we have used the fact that the relevant values of z are of the order of $z_0 \gg 1$. The (exponentially) large fluctuations of τ_W reflect a very wide distribution. Hence, we will describe these fluctuations in terms of the logarithm of τ_W. Moreover, for the remaining of this section we will adopt the dimensionless Wigner time

$$\tau = \frac{\tau_W}{\langle\tau_W\rangle} = 2N \frac{\tau_W}{t_{\mathrm{H}}}, \tag{3.23}$$

where $t_{\mathrm{H}} = 2\pi\hbar/\Delta$ is the Heisenberg time. Similarly to the calculation of the average log-conductance, we write

$$\begin{aligned}
\langle\ln\tau\rangle &= \frac{1}{\Delta} \left\langle \int_{-\Delta/2}^{\Delta/2} dE \, \ln^2\left[\frac{\gamma/(2\pi c)}{(E/c\Delta)^2 + \gamma^2/4}\right] \right\rangle \\
&\simeq \langle\ln\gamma\rangle + 2 + \ln\left(\frac{4c}{\pi}\right).
\end{aligned} \tag{3.24}$$

The first term in the right-hand side gives the dominant contribution and, to leading order in z_0, we have

$$\langle\ln\tau\rangle \simeq -\frac{z_0}{4}. \tag{3.25}$$

Therefore, in the asymptotic limit of $z_0 \gg 1$, the mean logarithmic of the conductance and the Wigner time are simply proportional to each other,

$$\langle\ln\tau\rangle = \frac{1}{4} \langle\ln g\rangle. \tag{3.26}$$

To investigate the fluctuations around this average value, we proceed in a way analogous to Eq. (3.19):

$$\langle \ln^2 \tau \rangle = \frac{1}{\Delta} \left\langle \int_{-\Delta/2}^{\Delta/2} dE \; \ln^2 \left[\frac{\gamma/(2\pi c)}{(E/c\Delta)^2 + \gamma^2/4} \right] \right\rangle$$

$$\simeq \langle \ln^2 \gamma \rangle \simeq \frac{z_0^2}{12}. \tag{3.27}$$

The variance of $\ln \tau$ is then given by

$$\mathrm{var}(\ln \tau) \;=\; \mathcal{C}_\tau(\Delta E{=}0) \;\simeq\; \frac{z_0^2}{48}. \tag{3.28}$$

The existence of correlations between the conductance and the Wigner time, as we presented in the Introduction (Fig.1.b), can be easily understood from Eqs. (3.2)-(3.3). Moreover, our resonant transmission model for localized transport allows us to quantify such correlations. For this purpose, instead of working with the cross-correlator (2.40), we define the logarithmic correlator

$$\mathcal{C}_{g\tau}(\Delta E) = \frac{\langle \delta \ln g(E + \Delta E) \; \delta \ln \tau(E) \rangle}{\langle (\delta \ln g)^2 \rangle^{1/2} \langle (\delta \ln \tau)^2 \rangle^{1/2}} \tag{3.29}$$

and calculate

$$\langle \ln g \ln \tau \rangle = \frac{1}{\Delta} \left\langle \int_{-\Delta/2}^{\Delta/2} dE \; \ln \left[\frac{\gamma^{(l)}\gamma^{(r)}}{(E/c\Delta)^2 + \gamma^2/4} \right] \ln \left[\frac{\gamma/(2\pi c)}{(E/c\Delta)^2 + \gamma^2/4} \right] \right\rangle$$

$$\simeq \left\langle \ln \left[\gamma^{(l)}\gamma^{(r)} \right] \ln \gamma \right\rangle + \left[\ln \left(\frac{2c}{\pi} \right) + 2 + 2\ln(c) \right] \left\langle \ln \left[\gamma^{(l)}\gamma^{(r)} \right] \right\rangle$$

$$+ 2[\ln(2c) + 1]\langle \ln \gamma \rangle$$

$$\simeq \frac{z_0^2}{4} - z_0 \left[\ln \left(\frac{2}{\pi} \right) + \frac{3}{2}\ln(2c) + 2 \right]. \tag{3.30}$$

To leading order in z_0 we have

$$\mathcal{C}_{g\tau}(\Delta E{=}0) \simeq \sqrt{\frac{6}{z_0}}, \tag{3.31}$$

showing that the cross-correlation decays slowly (not exponentially) with disorder.

In Table I we present our simulations in the localized regime for different disorder (W) and number of modes (N) in a stripe with aspect ratio $L_x/L_y = 4$. The results displayed show a qualitative agreement with the predictions of our resonant model [Eqs. (3.16), (3.9), (3.20), (3.25), (3.28), and (3.31)]. For the range of disorder that we are able to simulate, it is likely that the next-leading order in the large-z_0 asymptotic expansions of the above equations is required for a quantitative agreement. The $c-$dependent terms should be calculated consistently with the value of z_0 that best describes each sample. We will not attempt here this detailed comparison between the model and our numerical simulations because we would need a much better statistics than the one we dispose. The relationship (3.9) between the mean logarithmic conductance and its variance is only approximately verified in our numerical simulations. It has already been noticed [50] that in order to obtain the agreement with Eq. (3.9) one should simulate long stripes with weak disorder.

The fluctuations in $\ln g$ are larger than those in $\ln \tau$, despite the fact that in our resonant model the former depends linearly on z_0, while the latter goes quadratically with z_0. It is the difference in the prefactors that makes, for the values of the disorder that we have simulated, the fluctuations of $\ln g$ larger. One interesting aspect of the last column of Table I, the value of the cross correlations, is that the results of simulations seem to show an even slower dependence on z_0 than that of Eq. (3.31).

C. Energy and parametric correlations

The energy-dependent correlation functions for the log-conductance and log-Wigner time can be calculated from the resonant model along the same lines that we followed in the previous subsections. In particular, the various energy correlation lengths can be estimated from the initial curvature of the corresponding correlation functions. For the energy correlator of Eq. (3.18) we have

$$
\mathcal{C}_g''(\Delta E\!=\!0) \simeq \frac{4}{\Delta^2} \left\langle \frac{1}{\gamma c} \int_{-1/\gamma c}^{1/\gamma c} dx \, \frac{x^2 - 1}{(x^2 + 1)^2} \left\{ \ln \left[\gamma^{(l)} \gamma^{(r)} \right] - \ln \left(\frac{\gamma^2}{4} \right) - \ln \left(x^2 + 1 \right) \right\} \right\rangle
$$
$$
\simeq -\frac{8}{\Delta^2} \left\{ \frac{\pi}{2c} \left\langle \frac{1}{\gamma} \right\rangle + \left\langle \ln \left[\gamma^{(l)} \gamma^{(r)} \right] \right\rangle + 2 \ln(2c) - 1 \right\}. \tag{3.32}
$$

The term proportional to $\langle 1/\gamma \rangle$ gives the dominant contribution and its calculation is analogous to that of Eq. (3.22), yielding

$$
\mathcal{C}_g''(\Delta E\!=\!0) \simeq -\frac{2\pi^2}{c\Delta^2} \frac{1}{z_0} \, \exp \left(\frac{3}{4} z_0 \right). \tag{3.33}
$$

Assuming that the correlation function $\mathcal{C}_g(\Delta E)$ has approximately a Lorentzian form, its correlation energy will be related to the curvature at the origin through

$$
\Delta E_g^c \simeq \sqrt{-\frac{2\mathcal{C}_g(0)}{\mathcal{C}_g''(0)}} \simeq \Delta \frac{\sqrt{2c}}{\pi} z_0 \, \exp \left(-\frac{3}{8} z_0 \right). \tag{3.34}
$$

For the logarithmic correlation of the Wigner time we have (to leading order in z_0) the same curvature than for $\mathcal{C}_g(\Delta E)$ since $\ln \tau$ and $\ln g$ have the same energy dependence [Eqs. (3.2)-(3.3)]. The difference in the correlation lengths ΔE_g^c and ΔE_τ^c comes from the different values of the variances $\mathcal{C}_g(0)$ and $\mathcal{C}_\tau(0)$, yielding

$$
\Delta E_\tau^c \simeq \Delta \frac{1}{4\pi} \sqrt{\frac{c}{3}} z_0^{3/2} \, \exp \left(-\frac{3}{8} z_0 \right). \tag{3.35}
$$

Although the resonant model predicts that $\mathcal{C}_\tau(0)$ and $\mathcal{C}_g(0)$ have a quadratic and a linear dependence on z_0, respectively, we find numerically that $\mathrm{var}(\ln g)$ is always larger than $\mathrm{var}(\ln \tau)$ within the range of disorder and stripe lengths simulated. Therefore, we expect that $\Delta E_g^c > \Delta E_\tau^c$, which is indeed the behavior observed in Fig. 5. The energy-correlation length of $\mathcal{C}_{g\tau}$ is intermediate between ΔE_g^c and ΔE_τ^c. In all three cases, the correlation length shrinks exponentially with z_0, due to the fact that the conductance and Wigner-time peaks

become narrower with increasing disorder. This is the reason why we have used in Fig. 5 the energy rescaling appropriate for the parametric correlations of eigenphase velocities which also turns out to depend exponentially on z_0 (see below).

The correlation functions in the localized regime can be calculated with the aid of the resonant transmission model. The analysis is more involved for eigenphase velocities than for g or τ_W because we do not have a simple expression like (3.2) and (3.3) relating eigenphases to energy. However, there are obvious relations between correlators of eigenphases and Wigner times. The eigenphase velocity introduced in Eq. (2.1) is simply the diagonal part ($l = m$) of the sum defining the Wigner time correlator of Eq. (2.19). In particular, $C_\theta(\Delta E)$ and $C_\tau(\Delta E)$ are identical in one trivial limit of the localized case, namely, the $N = 1$, when we know the relation exactly (see Appendix B): Close to a resonance with energy E_ν, we have

$$\theta_\pm(E) \approx \pm\frac{\pi}{2} + \arctan[2(E - E_\nu)/\Gamma], \tag{3.36}$$

from which we recover the Breit-Wigner form of (3.3)

$$\tau_W(E) = \frac{\hbar}{2} \frac{\Gamma_\nu}{(E - E_\nu)^2 + \Gamma_\nu^2/4}. \tag{3.37}$$

In the large-N limit and for strongly disordered samples we can assume that the $\{\theta_l\}$ move almost rigidly, repelling each other simultaneously when a resonance occurs. Therefore, there is approximately no distinction between diagonal and off-diagonal correlations because all eigenphases follow a similar pattern of energy evolution This is confirmed in our numerical simulations by the close agreement between $\mathcal{C}_\tau$ and $\mathcal{C}_\theta$ over a wide energy range. The large fluctuations for the Wigner time translate into very large values of $C_\theta(0)$, as evident from Fig. 1.b. (Notice that the sharp steps of the phase shifts give rise to very large derivatives.) The broad distribution of eigenphases forces us to work with the logarithmic correlator

$$\mathcal{C}_\theta(\Delta E) = \left\langle \ln\left[\frac{d\theta_l(E + \Delta E)}{dE}\right] \ln\left[\frac{d\theta_l(E)}{dE}\right]\right\rangle - \left\langle \ln\left[\frac{d\theta_l(E)}{dE}\right]\right\rangle^2, \tag{3.38}$$

but still adopting the rescaling used in the metallic regime [Eq. (2.2)],

$$x = \Delta E \sqrt{\mathcal{C}_\theta(0)} \tag{3.39a}$$

$$c_\theta(x) = \mathcal{C}_\theta(\Delta E)/\mathcal{C}_\theta(0). \tag{3.39b}$$

The average in Eq. (3.38) is over energy E, disorder, and channel index l. In Fig. 5 we present $c_\theta(x)$ for in the localized regime (disorder $W = 4$). The universality found for the corresponding eigenphase velocity of the metallic regime is lost in a way consistent with our resonant model. On the other hand, when properly rescaled, we obtain an agreement between $c_\theta(x)$ and the Wigner time correlator.

IV. CONCLUSIONS

In this work we have studied parametric correlation functions in disordered quasi-one dimensional systems in the metallic and localized regimes. For this purpose we have considered the fluctuations in energy of the eigenphases of the scattering matrix, as well as fluctuations of the conductance and the Wigner time, and their cross correlation.

In the metallic regime, when disorder is weak and the fluctuations of the eigenphases $\{\theta_l\}$ are well described by Dyson's circular ensembles [11], the parametric correlations obtained from our numerical simulations follow closely the universal behavior discovered by Szafer, Altshuler, and Simons [15,16] for the spectra of chaotic and disordered systems. This finding is justified from a Brownian-motion model similar to that developed by Beenakker [33] for the energy spectrum. The Brownian-motion model also allows us to obtain the energy correlation function of the Wigner time in the large-energy asymptotic limit. We have compared these analytical results with our numerical simulations. Our simulations in the metallic regime display a strong correlation between the conductance and the Wigner time, which arises from the symmetry restrictions to the energy drift of the scattering matrix.

Transport in the localized regime is resonant-like and, therefore, its statistical properties are given by those of localized wave functions in the disordered stripe. From the well-known fact that wave functions are (1) localized around centers uniformly distributed in the sample (2) with inverse localization lengths following a Gaussian distribution, we recover the basic features observed in the simulations where disorder was strong. Our model is consistent with the standard log-normal distribution for the conductance and allowed us to estimate the typical energy correlation length of conductance fluctuations. The very large fluctuations of the Wigner time led us to study the distribution of its logarithm; the variance of this distribution was found to be related to that of the conductance. We also investigated the correlation between the conductance and the Wigner time as a function of disorder. The energy-dependent parametric correlations in the localized regime follow closely the behavior of the Wigner time.

An experimental check of some of the ideas developed in this work has become possible with the fabrication of very short insulating wires [52,53]. In particular, the Breit-Wigner line shape characteristic of resonant tunneling has been established and the statistics of peak position (as a function of Fermi energy or gate voltage) has been shown to display level repulsion [53]. This peculiar finding can be been understood within a resonant-tunneling picture if the observed peaks correspond to states well connected to the leads, which are confined to a small region in center of the stripe and which are therefore not necessarily separated from each other by distances much larger than the localization length. But the experimental study of short wires poses also the question of whether the single-particle approach that we have pursued in this work is valid. At least in a strictly one-dimensional sample it is known [54] that two-body potentials drive the system to a non-Fermi liquid behavior, leading to a more sensitive dependence on weak disorder [55]. Moreover, given the recent developments stressing the interplay between disorder and interactions in the localized regime [56–58], it would be interesting to extend the present study in order to incorporate the effects of electron-electron interactions in the energy-dependent parametric correlations.

ACKNOWLEDGMENTS

APPENDIX A: STATISTICAL PROPERTIES OF THE WIGNER-SMITH MATRIX

In this appendix we study the statistical distribution of the Wigner-Smith matrix in order to investigate more carefully the applicability of a unitary Brownian-motion model to the energy dependence of the scattering matrix.

For a small energy displacement, the evolution of the scattering matrix can be written as

$$S(E + \delta E) = S(E) \, \exp\left(i\delta K\right), \tag{A1}$$

where δK is required to be an infinitesimal Hermitian matrix to preserve the unitarity of S. To first order in δE, we can write

$$\delta K \;=\; -i \, S^\dagger \frac{dS(E)}{dE} \, \delta E \;=\; \frac{2N}{\hbar} \, Q \, \delta E. \tag{A2}$$

Consequently, considering now the form (2.7) of the allowed infinitesimal variations in the neighborhood of S, we can identify

$$Q \, \delta E = \frac{\hbar}{2N} \, Y^\dagger \, (\delta \tilde{H}) \, Y, \tag{A3}$$

showing that the eigenvalues of Q and $\delta \tilde{H}$ are proportional to each other. Moreover, if S has an isotropic distribution at a given E and remains isotropically distributed for each energy in the interval δE, one can see that this property should characterize Q as well. The isotropy of S and Q are related. We now try to determine which are the requirements on the probability distribution of Q necessary for the validity of the BMM [Eqs. (2.8)] at least in an approximate sense and for a sufficiently small δE.

We have investigated the probability distribution of the eigenvalues of Q by a numerical simulation on weakly-disordered metallic stripes. Under these conditions, the correlations of the eigenphases of S are well approximated by those of the CUE (or COE) ensemble [11], and the eigenphase velocity correlation agrees well with those found for chaotic Hamiltonian systems. In Fig. 6 we present the mean density of eigenvalues of Q and its nearest-neighbor spacing distribution (inset) for the cases without and with a time-symmetry breaking magnetic field. Notice that, within our convention, all eigenvalues of Q are positive, consistently with their interpretation as typical traversal times through the disorder region. Due to this symmetry requirement (that rules out the usual Gaussian ensembles), one of the simplest possible random-matrix description of Q is provided by the Laguerre ensembles. The observed eigenvalue density and the nearest-neighbor distribution (after unfolding [3]) are not incompatible with such an ensemble at first sight. Indeed, one can see a clear level repulsion and a good agreement with the Wigner's surmise of the appropriate symmetry class. Notice that although Q is not symmetric, the nearest-neighbor distribution in the time-reversal-symmetric case is given by the $\beta = 1$ Wigner surmise. This is because the submanifold of

allowed Q matrices in the presence of time-reversal symmetry can be mapped into that of the real symmetric ones by a transformation that leaves the eigenvalues unchanged [60]. It is important to remember that the other set of characteristic times, the energy derivatives of the phase shifts $\{d\theta_l/dE\}$ associated with the eigenchannels of S, *do not* exhibit nearest-neighbor repulsion. Both sets are, however, obviously related since their sum is simply τ_W.

For a disordered wire, S is not isotropic. (However, the circular ensembles give a good description of the phase shift fluctuations in the metallic regime.) Since the isotropy of S and Q are related, Q cannot be isotropic for a disordered wire. But one can hope that this does not matter for the spectral fluctuations of Q, in analogy with what happens for the spectral fluctuations of S. This lead us to consider a distribution for the Wigner-Smith matrix that is invariant under unitary (orthogonal) transformations, and to propose a simplified maximum-entropy ansatz [59,4]; in other words, we adopt a maximum-entropy distribution for Q, given the observed mean density of eigenvalues. This will yield a logarithmic interaction between eigenvalues and consequently the observed level repulsion. In the usual Coulomb gas analogy, one would have a certain (non-parabolic) confining potential for this ansatz giving the observed mean density of positive eigenvalues. The problem we face is then quite analogous to that of the probability distribution of the radial parameters of the transfer matrix [4,5].

It is well known that a maximum-entropy approach with an arbitrary confining potential leads to correlations between matrix elements [61]. The eigenvector isotropy assumption allows us to average over the unitary group [62,13], yielding

$$\langle Q_{ij}\rangle = \delta_{ij}\,\frac{\langle \text{Tr}Q\rangle}{N} \tag{A4a}$$

and

$$\langle Q_{ij}Q_{kl}\rangle = \frac{1}{N^2-1}\left[\delta_{ij}\delta_{kl}\left(\sum_{mn}\langle q_m q_n\rangle - \frac{1}{N}\sum_n\langle q_n^2\rangle\right) + \delta_{il}\delta_{jk}\left(\sum_n\langle q_n^2\rangle - \frac{1}{N}\sum_{mn}\langle q_m q_n\rangle\right)\right] \tag{A4b}$$

Above, brackets on the left-hand sides imply averages over the probability distribution of Q, while brackets on the right-hand sides indicate averages over the eigenvalue distribution. Equation (A4a) can be trivially set to zero once we suppress the constant drift of the eigenphases with energy (or use the convention $\langle\tau_W\rangle = 0$, like in subsection II.c). The non-vanishing correlations of Eq. (A4b) are

$$\langle Q_{ii}^2\rangle = \frac{1}{N+1}\left[(N-1)\langle q_1 q_2\rangle + 2\langle q_1^2\rangle\right], \tag{A5a}$$

$$\langle Q_{ii}Q_{jj}\rangle = \frac{1}{N+1}\left[N\langle q_1 q_2\rangle + \langle q_1^2\rangle\right] \qquad i \neq j, \tag{A5b}$$

$$\langle Q_{ij}Q_{ji}\rangle = \frac{1}{N+1}\left[\langle q_1^2\rangle - \langle q_1 q_2\rangle\right] \qquad i \neq j. \tag{A5c}$$

25

It is only in the case of the quadratic confinement potential that we have the GUE result $\langle q_1 q_2 \rangle = -\langle q_1^2 \rangle / N$ implying a vanishing correlation between different diagonal elements [Eq. (A5b)] and the usual correlation ($\langle Q_{ij} Q_{ji} \rangle = \langle q_1^2 \rangle / N$) between symmetric matrix elements [Eqs. (A5a) and (A5c)]. Other confining potentials, like the one compatible with the observed mean density, result in different two-point correlation functions $\langle q_1 q_2 \rangle$ and nonvanishing matrix element correlations in all Eqs. (A5).

If we assume that the eigenvectors of $\delta \tilde{H}$ are also isotropically distributed, Eqs. (A3) and (A5) show that there exist correlations between different matrix elements of $\delta \tilde{H}$. Therefore, Eqs. (2.8) cannot be verified exactly and their validity is actually approximate. On the other hand, the correlations of the type of Eq. (A5b) decrease with N and in the large N limit the maximum-entropy ensembles provide a local approximation to the Gaussian ones [63,3]. Therefore, it is only in the large N limit that the BMM for S can be appropriate.

Assuming a nearly Gaussian behavior and comparing Eqs. (A5a) and (A5c) with Eq. (2.8) allows the identifications

$$\delta t = (\delta E)^2 \tag{A6}$$

and

$$\frac{1}{f} = \frac{2\beta}{\hbar^2} \langle \mathrm{Tr} Q^2 \rangle, \tag{A7}$$

of the fictitious time and the friction coefficient of the BMM with the energy and Wigner-Smith matrix associated with the scattering process.

APPENDIX B: SCATTERING IN THE ONE-CHANNEL CASE

In this appendix we calculate the energy dependence of the eigenphases around a resonance for the one channel case. The starting point is the S-matrix expression [49]

$$S_{ab}(E) = e^{2i\varphi_a(E)} \delta_{ab} - 2\pi i \, e^{i\varphi_a(E) + i\varphi_b(E)} \sum_{\nu\mu} W_{a\mu}^*(E) [D^{-1}(E)]_{\mu\nu} W_{b\nu}(E), \tag{B1}$$

with

$$D_{\mu\nu}(E) = E\delta_{\mu\nu} - H_{\mu\nu} + i\pi \sum_c W_{c\mu}^*(E) W_{c\nu}(E). \tag{B2}$$

$W_{a\mu}(E)$ represents the overlap between the external wave functions (plane waves) and the internal eigenfunctions of H (for a time-reversal symmetric system we can choose $W_{a\mu}$ to be real). The usual approximation is to assume that the energy dependence of the phases $\varphi_a(E)$ and matrix elements $W_{a\mu}(E)$ is smooth over the interval where there are many resonances (poles) in $D^{-1}(E)$. Moreover, if $|W_{a\mu}|^2$ is typically much smaller than the average distance between poles, we can expand $[D^{-1}(E)]$ and perform a unitary transformation in the wave functions to obtain

$$S_{ab}(E) = \delta_{ab} - 2\pi i \sum_\nu \frac{W_{a\nu}^* W_{b\nu}}{E - E_\nu + i\Gamma_\nu/2} + O(\Gamma/\Delta), \tag{B3}$$

26

where $\Gamma_\nu = 2\pi \sum_c |W_{c\nu}|^2$. Now, specializing for a one-dimensional system (therefore $N = 1$) and looking at energies close to a certain resonance, we can get explicit expressions for the coefficients

$$r \approx 1 - \frac{2\Gamma_\nu^{(R)}/\Gamma_\nu}{1 - 2i(E - E_\nu)/\Gamma_\nu} \tag{B4a}$$

$$r' \approx 1 - \frac{2\Gamma_\nu^{(L)}/\Gamma_\nu}{1 - 2i(E - E_\nu)/\Gamma_\nu} \tag{B4b}$$

$$t \approx -\frac{\alpha}{1 - 2i(E - E_\nu)/\Gamma_\nu} \tag{B4c}$$

$$t' \approx -\frac{\alpha^*}{1 - 2i(E - E_\nu)/\Gamma_\nu}, \tag{B4d}$$

with $\alpha = 4\pi W_{L\nu}^* W_{R\nu}/\Gamma_\nu$. Notice that (B3) keeps S unitary only to lowest order in Γ/Δ.

It is useful to introduce the following parameterization for S:

$$r = \sqrt{R}\ e^{i\eta + \chi}$$
$$r^* = \sqrt{R}\ e^{\eta - \chi}$$
$$t = i\sqrt{T}\ e^{i\eta + i\kappa}$$
$$t^* = i\sqrt{T}\ e^{i\eta - i\kappa}, \tag{B5}$$

with $R + T = 1$. The various quantities appearing above can be determined through Eq. (B4); in particular,

$$\eta(E) \approx \arctan[2(E - E_\nu)/\Gamma_\nu] \tag{B6}$$

and

$$T(E) \approx \frac{|\alpha|^2}{1 + 4(E - E_\nu)^2/\Gamma_\nu}. \tag{B7}$$

For time-reversal symmetric systems ($\kappa = 0$), it is easy to find an expression for the eigenphases of S in terms of the new parameters, namely,

$$\theta_\pm = \eta \pm \arctan\left(\sqrt{\frac{T}{R}}\right), \quad \mathrm{mod}(\pi). \tag{B8}$$

Using Eqs. (B6) and (B7), we then have

$$\theta_\pm(E) \approx \arctan[2(E - E_\nu)/\Gamma_\nu] \pm \arctan\left[\frac{|\alpha|^2}{1 - |\alpha|^2 + 4(E - E_\nu)^2/\Gamma_\nu}\right]^{1/2}, \quad \mathrm{mod}(\pi). \tag{B9}$$

Notice that, in general, $\Gamma_R \neq \Gamma_L$ and $|\alpha|^2 < 1$. This means that the second term on the r.h.s of Eq. (B9) varies slower than the first and the difference between eigenphases around a resonance is approximately π [Eq. (3.36)].

Note added: While finishing this manuscript, we learnt from C. Beenakker that an exact random matrix description of the distribution of the Wigner-Smith matrix Q can be obtained in the case that either S remains distributed following the Dyson circular ensembles as E varies, or the underlying Hamiltonian is a member of the Gaussian ensembles. This can be applied to ballistic chaotic cavities, but not to the disordered wires which we study. However, the result is very similar to the maximum-entropy description which we proposed in the Appendix A, notably as far the level repulsion is concerned. The extension of the derivation made by Beenakker and co-workers from the ballistic cavity to the disordered wire should allow us to see what corrections to the maximum-entropy ansatz proposed in Appendix A are required.

REFERENCES

[1] K. B. Efetov, Adv. Phys. **32**, 53 (1983).

[2] B. L. Altshuler and B. I. Shklovskiĭ, Zh. Eksp. Teor. Fiz. **91**, 220 (1986) [Sov. Phys. JETP **64**, 127 (1986)].

[3] O. Bohigas, in *Chaos and Quantum Physics* (North-Holland, New York, 1991) ed. by M.-J. Giannoni, A. Voros, and J. Zinn-Justin.

[4] A. D. Stone, P. A. Mello, K. A. Muttalib, and J.-L. Pichard, in *Mesoscopic Phenomena in Solids* (North-Holland, Amsterdam, 1991), edited by B. L. Altshuler, P. A. Lee, and R. A. Webb.

[5] C. W. J. Beenakker, Phys. Rev. B **47**, 15763, (1993).

[6] J. J. M. Verbaarschot, H. A. Weidenmüller, and M. R. Zirnbauer, Phys. Rep. **129**, 367 (1985).

[7] S. Iida, H. A. Weidenmüller, and J. A. Zuk, Annals of Phys. **200**, 219 (1990).

[8] H. U. Baranger and P. A. Mello, Phys. Rev. Lett. **73**, 142 (1994).

[9] R. A. Jalabert, J.-L. Pichard, and C. W. J. Beenakker, Europhys. Lett. **27**, 255 (1994).

[10] Z. Pluhǎr, H. A. Weidenmüller, J. A. Zuk, and C. H. Lewenkopf, Phys. Rev. Lett. **73**, 2115 (1994); Z. Pluhǎr, H. A. Weidenmüller, J. A. Zuk, C. H. Lewenkopf, and F. J. Wegner, Annals of Phys. **243**, 1 (1995).

[11] R. A. Jalabert and J.-L. Pichard, J. Phys. (France) **5**, 287 (1995). Notice the typographic mistake in Eq. (4.5): the confining potential should read $V(\lambda) = [N + (2-\beta)/\beta] \ln(1+\lambda)$.

[12] F. J. Dyson, J. Math. Phys. **3**, 140 (1962).

[13] M. L. Mehta, *Random Matrices*, 2nd ed. (Academic Press, San Diego, 1991).

[14] R. Blümel and U. Smilansky, Phys. Rev. Lett. **64**, 241 (1989).

[15] A. Szafer and B. L. Altshuler, Phys. Rev. Lett. **70**, 587 (1993); B. D. Simons, A. Szafer, and B. L. Altshuler, Pis'ma Zh. Eksp. Teor. Fiz. **57**, 268 (1993) [JETP Lett. **57**, 276 (1993)].

[16] B. D. Simons and B. L. Altshuler, Phys. Rev. Lett. **70**, 4063 (1993); Phys. Rev. B **48**, 5422 (1993).

[17] M. Faas, B. D. Simons, X. Zotos, and B. L. Altshuler, Phys. Rev. B **48**, 5439 (1993).

[18] E. R. Mucciolo, R. B. Capaz, B. L. Altshuler, and J. D. Joannopoulos, Phys. Rev. B **50**, 8245 (1994).

[19] B. D. Simons, A. Hashimoto, M. Courtney, D. Kleppner and B. L. Altshuler, Phys. Rev. Lett. **71**, 2899 (1993).

[20] N. Lehmann, D. V. Savin, V. V. Sokolov, and H.-J. Sommers, Physica D **86**, 572 (1995).

[21] Y. V. Fyodorov and H.-J. Sommers, Phys. Rev. Lett. **76**, 4709 (1996).

[22] V. A. Gopar, P. A. Mello, and M. Büttiker, Phys. Rev. Lett. **77**, 3005 (1996).

[23] F. T. Smith, Phys. Rev. **118**, 349 (1960); **119**, 2098 (1960).

[24] D. S. Fisher and P. A. Lee, Phys. Rev. B **23**, 6851, (1981).

[25] P. A. Lee and D. S. Fisher, Phys. Rev. Lett. **47**, 882, (1981).

[26] H. U. Baranger, D. P. DiVincenzo, R. A. Jalabert, and A. D. Stone, Phys. Rev. B **44**, 10637 (1991).

[27] R. Landauer, Philos. Mag. **21**, 863 (1970); M. Büttiker, Phys. Rev. Lett. **57**, 1761 (1986).

[28] B. A. Muzykantskii and D. E. Khmelnitskii, Phys. Rev. B **51**, 5480 (1995).

[29] The COE and CUE theoretical curves were obtained according to Eqs. (2.3) after numerical diagonalization of 500×500 matrices of the form $H(X) = H_1 \cos(X) + H_2 \sin(X)$, where H_1 and H_2 were drawn from the proper Gaussian ensemble. The averages were performed over the 100 central eigenvalues and 50 realizations.

[30] B. D. Simons, P. A. Lee, and B. L. Altshuler, Phys. Rev. Lett. **72**, 64 (1994); Nucl. Phys B **409**, 487 (1993).

[31] A. V. Andreev, O. Agam, B. D. Simons, and B. L. Altshuler, Phys. Rev. Lett. **76**, 3947 (1996).

[32] A. M. S. Macêdo, Phys. Rev. E **50**, R659 (1994).

[33] C. W. J. Beenakker, Phys. Rev. Lett. **70**, 4126 (1993).

[34] F. J. Dyson, J. Math. Phys. **3**, 1191 (1962).

[35] A. Pandey and P. Shukla, J. Phys. A **24**, 3907, (1991); A. Pandey, R. Ramaswamy, and P. Shukla, Pramana J. Phys. (India) **41**, L75 (1993).

[36] J. Rau, Phys. Rev. B **51**, 7734 (1995).

[37] K. Frahm and J.-L. Pichard, J. Phys. I (France) **5**, 847 (1995); **5**, 877 (1995).

[38] B. Sutherland, Phys. Rev. A **4**, 2019 (1971); **5**, 1372 (1972).

[39] For a solution for the case of Hamiltonian eigenvalues when $\beta = 2$, see C. W. J. Beenakker and B. Rejaei, Physica A **203**, 60 (1994).

[40] F. J. Dyson, J. Math. Phys. **13**, 90 (1972).

[41] R. Blümel and U. Smilansky, Phys. Rev. Lett. **60**, 477 (1988); Physica D **36**, 111 (1989).

[42] H. U. Baranger, R. A. Jalabert, and A. D. Stone, Chaos, **3**, 665 (1993).

[43] B. Eckhardt, Chaos, **3**, 613 (1993).

[44] C. H. Lewenkopf and H. A. Weidenmüller, Ann. Phys. (N.Y.) **212**, 53 (1991).

[45] E. Akkermans and G. Montambaux, Phys. Rev. Lett. **68**, 642 (1992).

[46] E. Doron and U. Smilansky, Phys. Rev. Lett. **68**, 1255 (1992); Nonlinearity **5**, 1055 (1992).

[47] P. A. Lee, A. D. Stone, and H. Fukuyama, Phys. Rev. B**35**, 1039 (1987).

[48] A. M. Lane and R. G. Thomas, Rev. Mod. Phys. **30**, 257 (1958).

[49] C. Mahaux and H. A. Weidenmüller, *Shell-Model Approach to Nuclear Reactions* (North-Holland, Amsterdam, 1969).

[50] Y. G. Avishai, J.-L. Pichard, and K. A. Muttalib, J. Phys. (France) **3**, 2343, (1993).

[51] J.-L. Pichard in *Quantum Coherence in Mesoscopic Systems*, edited by B. Kramer, NATO ASI Series B 254 (Plenum, New York, 1991).

[52] F. Ladieu, D. Mailly, and M. Sanquer, J. Phys. (France) **3**, 2321, (1993).

[53] W. Poirier, M. Sanquer, and D. Mailly, in *Hopping and Related Phenomena VI* (Jerusalem, 1995).

[54] H. J. Schulz in *Mesoscopic Quantum Physics*, edited by E. Akkermans, G. Montambaux, J.-L. Pichard, and J. Zinn-Justin (Elsevier, Amsterdam, 1995).

[55] C. L. Kane and M. P. A. Fisher, Phys. Rev. B **46**, 15233 (1992).

[56] D. L. Shepelyansky, Phys. Rev. Lett. **73**, 2067 (1994).

[57] D. Weinman, A. Müller-Groeling, J.-L. Pichard, and K. Frahm, Phys. Rev. Lett. **75**, 1598 (1995).

[58] F. von Oppen, T. Wettig, and J. Müller, Phys. Rev. Lett. **75**, 1598 (1995).

[59] R. Balian, Nuovo Cim. B **57**, 183 (1968).

[60] P. A. Mello, private communication.

[61] N. Ullah and C. E. Porter, Phys. Lett. **6**, 301 (1963).

[62] P. A. Mello, J. Phys. A **23**, 4061 (1990).

[63] A. M. Ozorio de Almeida, *Hamiltonian Systems: Chaos and Quantization* (Cambridge University Press, 1988).

W	N	$\langle \ln g \rangle$	$\langle (\delta \ln g)^2 \rangle$	$\langle \tau \rangle$	$\langle \ln \tau \rangle$	$\langle (\delta \ln \tau)^2 \rangle$	$\mathcal{C}_{g\tau}$
4	14	-4.1	7.0	1.3	-0.01	0.40	0.67
4	10	-6.2	9.2	1.2	-0.21	0.62	0.74
5	14	-9.8	8.6	1.2	-0.43	0.71	0.62
5	10	-9.0	13.8	1.1	-0.49	0.79	0.60
6	14	-16.1	29.1	1.2	-0.69	0.80	0.53
6	10	-17.2	28.8	1.3	-0.99	0.93	0.55
7	14	-24.5	39.3	1.1	-0.92	0.81	0.52

TABLE I. Simulations of stripes in the localized regime with aspect ratio $L_x/L_y = 4$, mean disorder W, and number of channels N. The averages are over energy and impurity configuration. $\langle \ln g \rangle$ and $\langle (\delta \ln g)^2 \rangle$ are the mean logarithmic conductance and its variance, respectively. The mean Wigner time $\langle \tau \rangle$ has been normalized to its average value $\pi \hbar / N \Delta$, and therefore the fifth column checks the validity of Eq. (3.20). $\langle \ln \tau \rangle$ and $\langle (\delta \ln \tau)^2 \rangle$ are the mean logarithmic Wigner time and its variance, respectively. The last column is the value of the cross correlator between the conductance and Wigner time calculated as in Eq. (3.29).
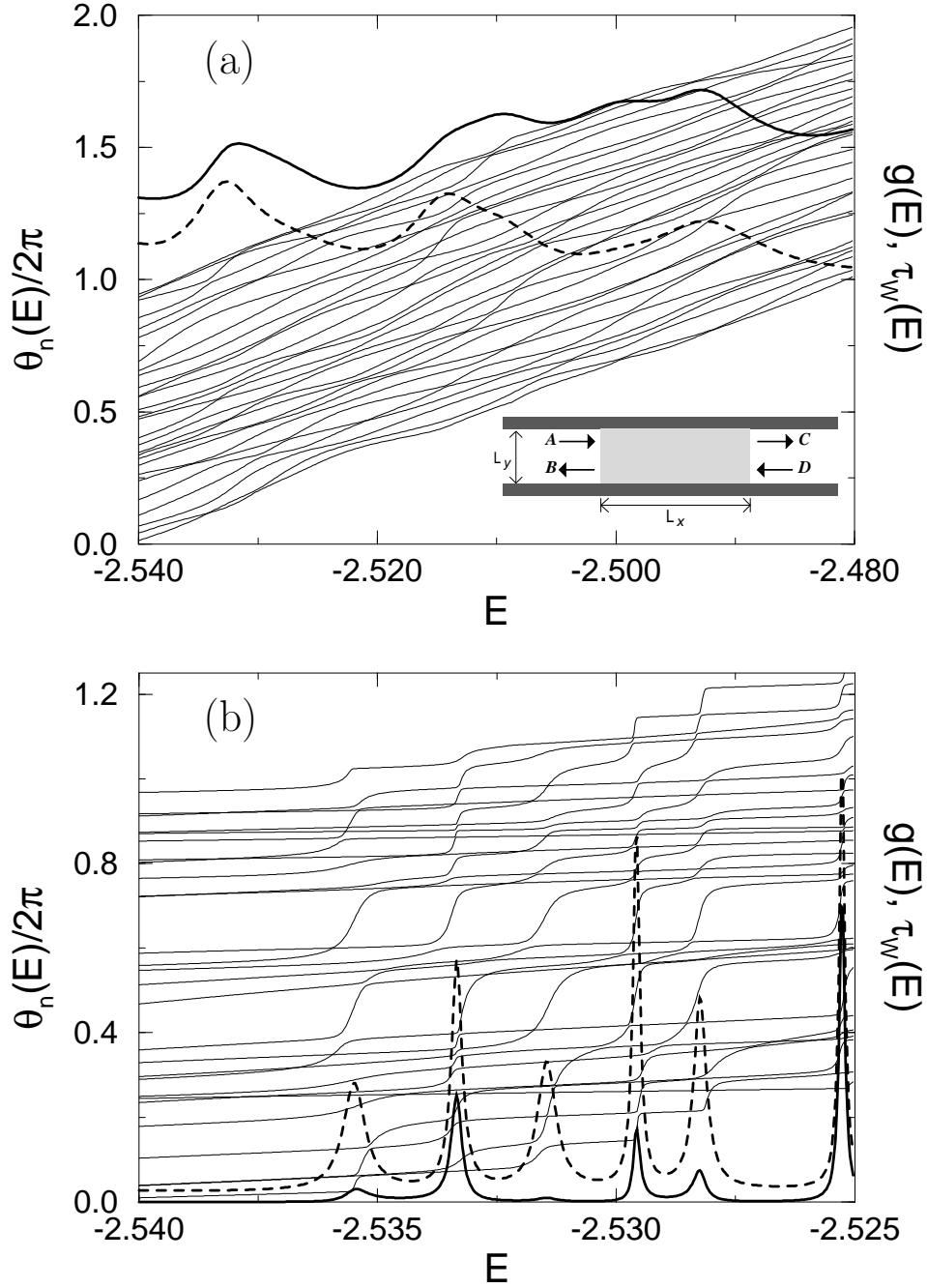
FIG. 1. Energy dependence of the phase shifts for a quasi-1D disordered stripe (inset) in the metallic (a) and localized (b) regimes. The conductance and the Wigner time (thick solid and dashed lines, respectively, both in arbitrary units) are smooth functions in the metallic regime and exhibit a resonant structure in the localized regime. The energy range in (b) is chosen to facilitate the visualization of the resonances. Note the strong correlation between g and τ_W.
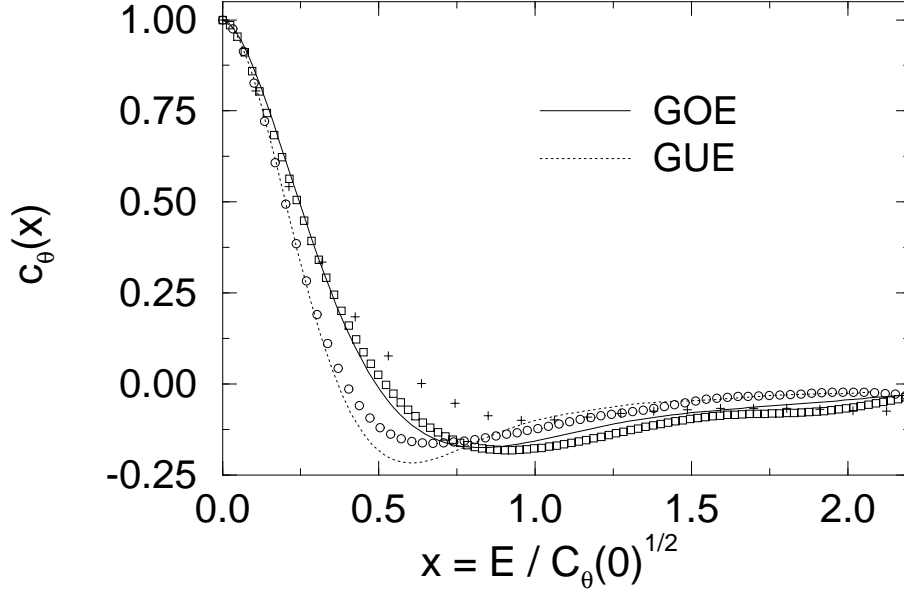
FIG. 2. Eigenphase velocity correlator for the metallic regime according to the definitions of Eqs. (2.1) and (2.2). The weakly-disordered metallic case (W=1 in Anderson units) with (circles) and without magnetic field (squares) shows a good agreement with the universal curves characteristic of the GUE and GOE, respectively. Increasing the disorder (W=2, no magnetic field, pluses) reduces the range of agreement with the universal curve.
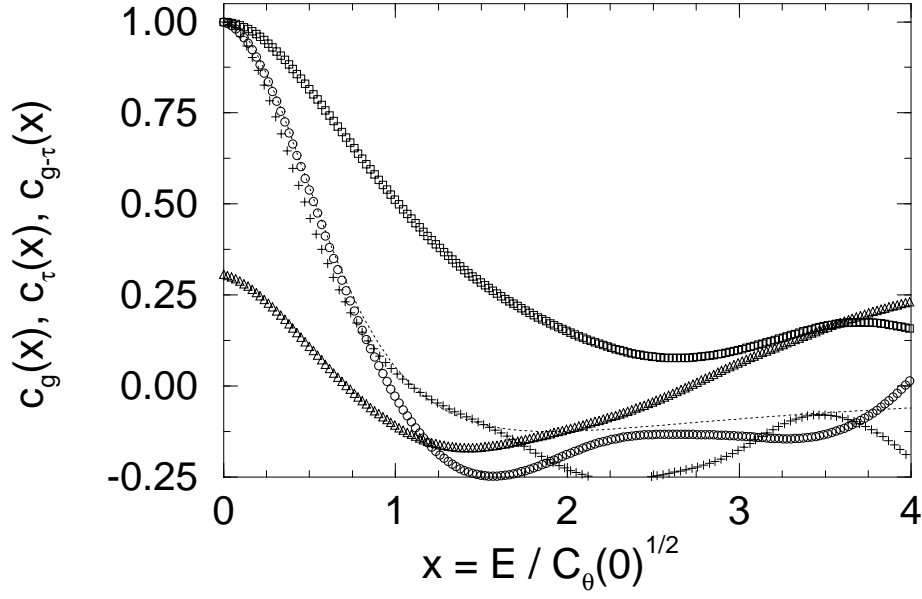
FIG. 3. Autocorrelations of the conductance g (square) and the Wigner time τ_W (circle) and the cross-correlation between g and τ_W (triangle) for the metallic case without magnetic field. The autocorrelator of Wigner times in the presence of a magnetic field is also plotted (pluses). The dotted curve is a plot of Eq. (2.29).
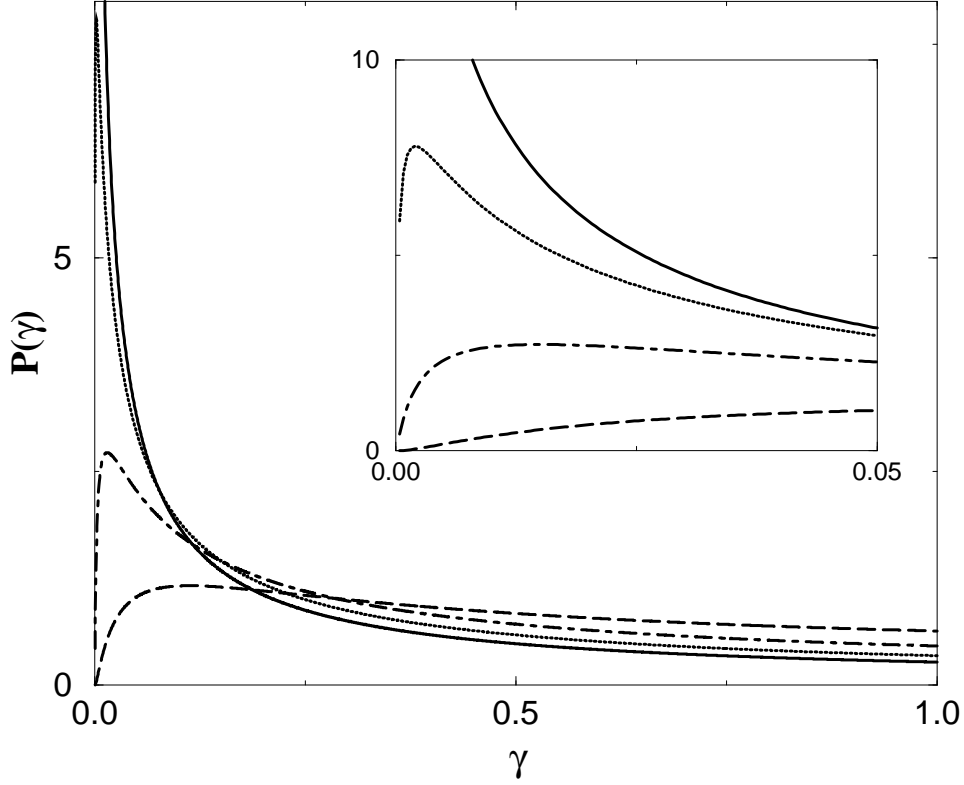
FIG. 4. Probability distribution for the dimensionless total width γ for increasing disorder (parameterized by z_0). Dashed line: $z_0 = 4$, corresponding to the case shown in Fig. (1).b; dash-dotted: $z_0 = 6$; dotted: $z_0 = 8$; solid line: $z_0 = 10$. Inset: blow up of the small γ region showing how the most probable value of the distribution moves towards the origin with increasing disorder.
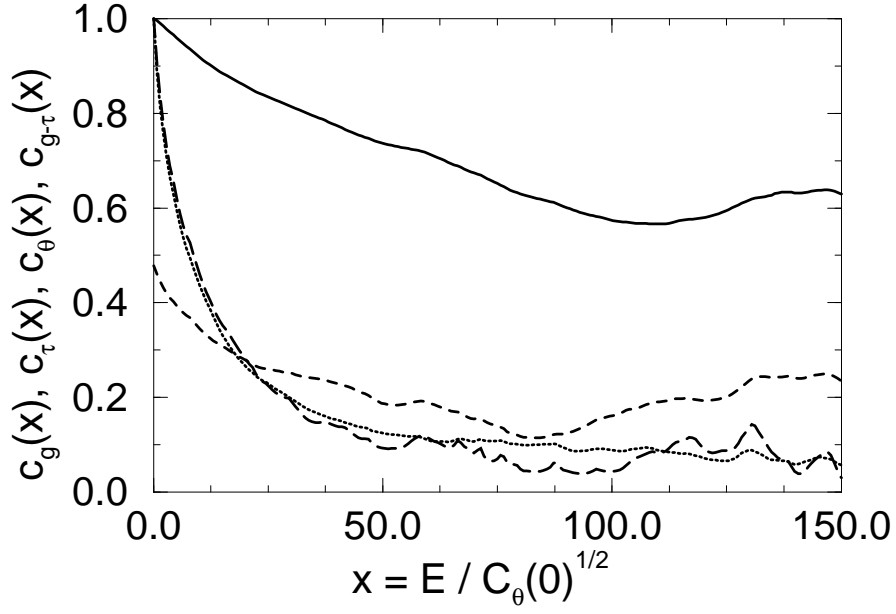
FIG. 5. Logarithmic autocorrelations of the conductance (solid), Wigner time (dotted), and eigenphase velocity (long-dashed) for the strongly localized case ($W=4$ in Anderson units) without magnetic field. The cross-correlation between g and τ_W is shown by the thick short-dashed curve. The use of the logarithmic was required in view of the broad distributions of g and τ_W (see text).
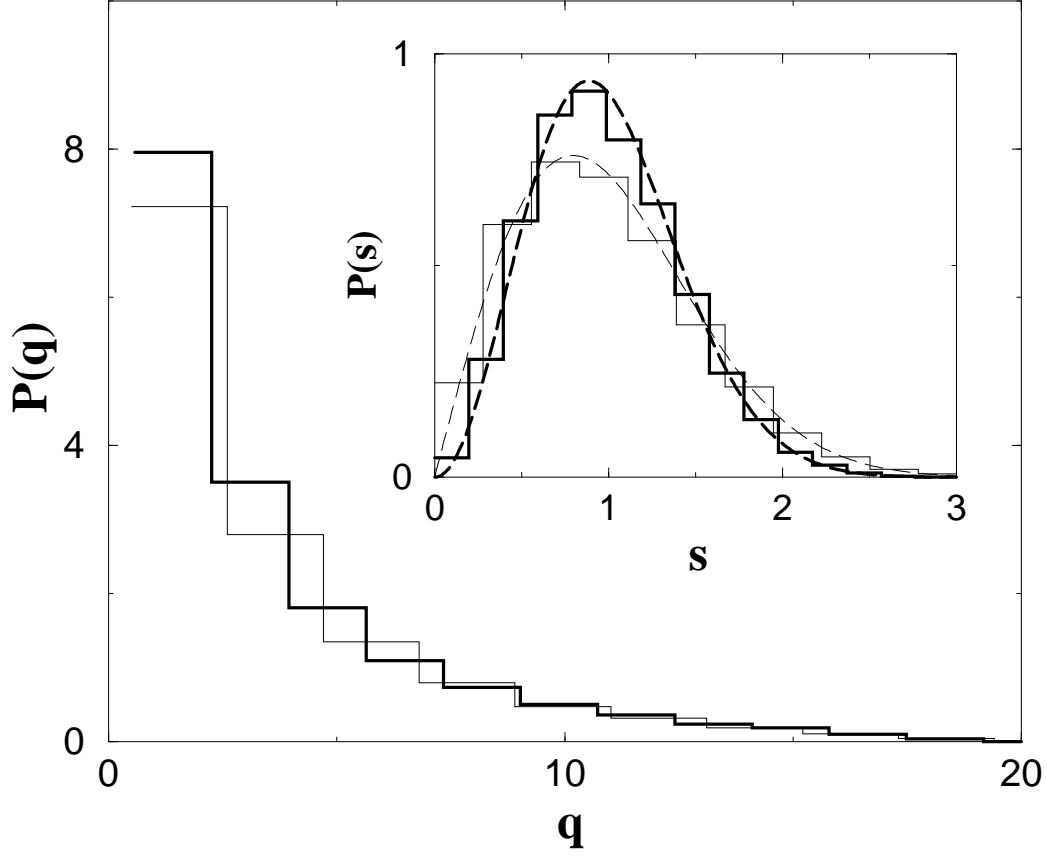
FIG. 6. Distribution of the eigenvalues of the Wigner-Smith matrix in the weakly-disordered metallic regime. The thick and thin lines correspond to the presence or absence of a magnetic field, respectively. The inset shows the nearest-neighbor spacing histogram for the same eigenvalues (similar convention for the line widths). The Wigner surmises for the GUE and GOE (thick and thin dashed lines, respectively) are shown for comparison.